Electronic structure and stability of the ferrimagnetic ordering in double perovskites

I. V. Solovyev*
JRCAT-Angstrom Technology Partnership, c/o AIST, Central 4, 1-1-1 Higashi, Tsukuba, Ibaraki 305-0046, Japan
and Institute of Metal Physics, Russian Academy of Sciences, Ekaterinburg GSP-170, Russia
(Received 16 November 2001; published 4 April 2002)

Using results of first-principles band structure calculations and a model tight-binding approach, we investigate the local stability of the half-metallic ferrimagnetic (FiM) states in double perovskites Sr_2FeMO_6 (M = Mo, Re, and W). In ordered compounds, a generalized double-exchange (DE) mechanism operating in the metallic minority-spin channel, in a hybrid Fe-M-derived t_{2g} band, always competes with the strong antiferromagnetic superexchange (SE) interactions in the Fe sublattice mediated by virtual electron hoppings into the unoccupied $M(d)$ states. In the local-spin-density approximation (LSDA), the SE mechanism largely prevails and the FiM phase is unstable with respect to a noncollinear spin-spiral alignment. The situation appears to be more generic. So, the onsite Coulomb repulsion between the Fe($3d$) electrons (ΔU) on the top of the LSDA picture suppresses the SE interactions but may also modify some of the DE interactions through the change of the Fe-M hybridization. The total change of the electronic structure, caused by ΔU alone, does not explain the local stability of the FiM state. Therefore, we conclude that the FiM phase cannot be stabilized by purely electronic mechanisms. According to our scenario, that is exactly the situation realized in Sr_2FeWO_6. An interpretation of the experimental FiM ordering observed in Sr_2FeMoO_6 and Sr_2FeReO_6 should require an additional mechanism, which destroys the half-metallic character of the electronic structure and suppresses the saturation moment. We consider two possibilities: the alternating breathing distortions of the FeO_6 and MO_6 octahedra, and the antisite (Fe-M interchange) disorder. In the former case, the oxygen displacement towards the Fe-sites leads to the partial depopulation of the majority-spin Fe(e_g) band and thereby activates an effective channel for the ferromagnetic DE interactions, similar to colossal-magnetoresistive manganites. In the latter case, the FiM ordering can be stabilized by SE interactions of a small (less than 10%) amount of Fe impurities with the host atoms. We discuss possible implications of these scenarios to different compounds with emphasis on their magnetic and optical properties.

DOI: 10.1103/PhysRevB.65.144446 PACS number(s): 75.30.Et, 75.50.Gg, 72.25.Ba, 71.20.Be

I. INTRODUCTION

Recently, ordered double perovskites (DP) Sr_2FeMO_6, and especially Sr_2FeMoO_6 and Sr_2FeReO_6, have received a lot of attention. Although the materials themselves were known for several decades,[1] the renewed interest in these systems was spurred by two important observations. (i) They exhibit fairly large intergrain-tunneling magnetoresistance effect.[2,3] Therefore, from the practical point of view the main focus of the research activity was shifted towards polycrystalline specimens, while the behavior of Sr_2FeMO_6 single crystals presents mainly an academic interest and is important to clarify basic properties of these compounds.[4] (ii) Both Sr_2FeMoO_6 and Sr_2FeReO_6 have fairly high Curie temperature (T_C=415 K and 401 K, respectively). This is a great advantage over the colossal-magnetoresistive manganites, which makes the DP suitable candidates for technological applications in magnetoresistive devices operating at room temperature.

From the theoretical point of view, it is frequently believed that the behavior of DP presents an example of ''simple physics,'' and that the unique properties of Sr_2FeMoO_6 and Sr_2FeReO_6 are related to the fully spin-polarized half-metallic (HM) electronic structure obtained in band calculations for the ferromagnetic (FM) state.[2,3] Perhaps, it is more correct to call this state ferrimagnetic (FiM), because the hybridization between d orbitals of the Fe and M atoms induces nonvanishing spin magnetic moments also at the M sites, which are aligned antiferromagnetically with respect to the spin moments of Fe.[5–7]

There are several experimental facts that do not quite fit into this picture.

(i) Even in Sr_2FeMoO_6 and Sr_2FeReO_6, the saturation magnetization is always lower than the ideal value expected for the 100% polarized HM electronic state. The record (ideal) values of the spin magnetic moments obtained in Sr_2FeMoO_6 and Sr_2FeReO_6 are $3.7(4.0)\mu_B$ and $2.7(3.0)\mu_B$, respectively.[3,8,9] It is believed, however, that the saturation moments can be further increased by a routine improvement of the quality of samples.

(ii) There is another material, Sr_2FeWO_6, which is expected to be very similar to Sr_2FeMoO_6 (also from the viewpoint of band calculations,[6] which predict the HM behavior in the FiM state also for Sr_2FeWO_6). However, according to the experimental data, Sr_2FeWO_6 is an antiferromagnetic (AFM) insulator with very low Néel temperature ($T_N \sim 16$–37 K).[10,11]

(iii) There is also an opposite example, Ca_2FeReO_6, which is a ferrimagnet with an extremely high transition temperature (538 K) and at the same time—an insulator.[12]

Surprisingly that despite such an enormous interest in the HM behavior associated with the FiM phase and numerous implications of this picture, there was no detailed theoretical analysis of the problem. To begin with, how do we know that the FiM state is the magnetic ground state of Sr_2FeMO_6? According to recent total energy calculations,[6] the FiM state

has lower energy than an AFM state for *all three* compounds Sr_2FeMoO_6, Sr_2FeReO_6, and Sr_2FeWO_6, both in the local-spin-density approximation (LSDA) and in its extension—the generalized gradient approximation (GGA). In order to explain an exceptional place of Sr_2FeWO_6 in this row, the authors of Ref. 6 had to rely on a delicate balance of onsite Coulomb correlations (which should turn into the AFM regime only Sr_2FeWO_6, but not Sr_2FeMoO_6 or Sr_2FeReO_6). Suppose that this is the case, and the FiM state may indeed have lower energy under some circumstances. Then, how do we know that it is a *minimum* of the total energy (rather than a maximum) and that the system is stable with respect to a more complicated noncollinear spin-spiral alignment that may be the true magnetic ground state?

The present work is aimed at dealing with these kinds of questions for the double perovskites. In Sec. II, we will describe a concept of the magnetic phase stability and explain its main advantage with respect to the conventional total energy calculations (that is basically the analysis of second derivatives of the total energy versus the total energies themselves). In Secs. III and IV, we will present results of this analysis for the ordered DP and argue that the HM electronic structure is *incompatible* with the magnetic ground state of these systems and that the FiM phase is *unstable*. In Sec. V we will discuss several scenarios, which can stabilize the FiM ordering (but only at the cost of demolishing of the HM character of the electronic structure—that is an irony of the situation). In Sec. VI we will show how these changes of the electronic structure are (or should be) reflected in the change of spectroscopic (optical and magneto-optical) data. Finally, in Sec. VII we will give a conclusion and try to present a new classification for the $Sr_2Fe\mathit{M}O_6$ compounds by putting everything ''upside-down'': we will argue that nearly antiferromagnetic Sr_2FeWO_6 reflects a normal behavior for the ordered DP, while describing the properties of Sr_2FeMoO_6 or Sr_2FeReO_6 should require an additional physics.

II. TOTAL ENERGIES VERSUS PARAMETERS OF MAGNETIC INTERACTIONS

Let us start with an equilibrium spin configuration $\mathcal{M}^0=\{\mathbf{e}_i^0\}$ that is characterized by the directions $\mathbf{e}_i^0=(\sin\theta_i^0\cos\phi_i^0,\sin\theta_i^0\sin\phi_i^0,\cos\theta_i^0)$ of the spin magnetic moments at each site (i) of the lattice. For example, in the FiM state of $Sr_2Fe\mathit{M}O_6$ we have $\mathbf{e}_{\mathrm{Fe}}=(0,0,1)$ for all Fe sites and $\mathbf{e}_M=(0,0,-1)$ for all M sites. The total energy of the system corresponding to $\mathcal{M}^0$ is denoted as E_0. Then, let us consider the spin rotations $\{\boldsymbol{\delta\varphi}_i\}$ to the new (nonequilibrium) configuration $\mathcal{M}=\{\mathbf{e}_i\}$ with the directions $\mathbf{e}_i=\mathbf{e}_i^0+[\boldsymbol{\delta\varphi}_i\times\mathbf{e}_i^0]-\frac{1}{2}(\boldsymbol{\delta\varphi}_i)^2\mathbf{e}_i^0$. The new total energy is given by

$$E(\mathcal{M})=E_0+\Delta E,$$

and in the second order of $\{\boldsymbol{\delta\varphi}_i\}$ the change ΔE can be mapped onto the Heisenberg model[13]

$$\Delta E=-\frac{1}{2}\sum_{im}J_m[\mathbf{e}_i\cdot\mathbf{e}_{i+m}-\mathbf{e}_i^0\cdot\mathbf{e}_{i+m}^0]. \tag{1}$$

All previous studies of the ordered DP focused mainly on the comparison of E_0 for a limited number of collinear (typically, ferrimagnetic and antiferromagnetic) spin configurations.[6,14,15] In this work we will primarily concentrate on the behavior of $\{J_m\}$, which are nothing but the second derivatives of the total energy with respect to $\{\boldsymbol{\delta\varphi}_i\}$. Being complementary to E_0, these parameters give us very important information about the local stability (and also the instability) of the FiM phase, which will significantly alter our view of the origin of ferrimagnetism in $Sr_2Fe\mathit{M}O_6$.

In the density-functional theory both E_0 and $\{J_m\}$ are the ground-state properties,[16] and in principle must be related to each other. However, the exact relation, though can be established for a number of model examples,[17,18] is not generally known.

From the computational point of view the calculations of E_0 and $\{J_m\}$ for the DP pose several problems. On the one hand, the distribution of the spin-magnetization density is rather complex and can significantly deviate from the spherical one, especially around the M and O sites. All details of this distribution cannot be properly described at the level of the atomic spheres approximation (ASA) underlying the linear muffin-tin orbital method (LMTO),[19] which we intend to use in the present work. These details are very important for the total energy calculations and the values of E_0 obtained in the ASA-LMTO approach may not be very reliable in comparison with results of more rigorous full-potential calculations. Therefore, we do not discuss them here.

There are also several questions related to the choice of the exchange-correlation functional, to which E_0 appears to be extremely sensitive. For example, in GGA the FiM state acquires an additional energy gain coming from the magnetic polarization of the M sites, in comparison with results of more traditional LSDA. Although GGA yields somewhat better values for the total energies in the DP,[6] it is not easy to find a good physical explanation to this fact because from the viewpoint of the single-particle electronic structure, the GGA and LSDA results look almost identical.

On the other hand, the straightforward calculations of $\{J_m\}$ on the basis of full-potential techniques are not feasible at the present stage, at least for such large systems as the DP. For these purposes the ASA-LMTO method still remains the only possibility. Fortunately, for the practical calculations of $\{J_m\}$ one can use the local-force theorem,[13,16] which means that instead of laborious total energy calculations, requiring very high accuracy, ΔE can be found from the change of the single-particle energies with a frozen Kohn-Sham potential. Therefore, if the main details of the single-particle electronic structure of the DP can be captured by the ASA-LMTO method, it is reasonable to expect that results of the ASA-LMTO calculations for $\{J_m\}$ may be also reliable.

The practical calculations of $\{J_m\}$ can be performed along two lines, each of which has its own merits and demerits. In this work we will employ both of them. The first one is to use the perturbation theory based on the Green-function technique, which allows us to obtain the analytical expression for J_m,[13]

TABLE I. Size of atomic radii used in calculations (in atomic units).

Compound	Sr/Ba	Fe	*M*	O
Sr_2FeMoO_6	3.733	2.743	3.011	1.968
Ba_2FeMoO_6	3.888	2.778	3.041	1.951
Sr_2FeReO_6	3.728	2.744	3.022	1.968
Sr_2FeWO_6	3.724	2.738	3.059	1.960

$$J_m = \frac{1}{2\pi}\mathrm{Im}\int_{-\infty}^{\varepsilon_F} d\varepsilon\ \mathrm{Tr}_L\{\Delta_{\mathrm{ex}}^0 \hat{\mathcal{G}}_{0m}^{\uparrow}(\varepsilon)\Delta_{\mathrm{ex}}^m \hat{\mathcal{G}}_{m0}^{\downarrow}(\varepsilon)\}, \qquad (2)$$

where $\hat{\mathcal{G}}_{0m}^{\uparrow,\downarrow}$ are the elements of one-electron Green function between sites 0 and m for the majority ($\uparrow$) and minority ($\downarrow$) spin states; Δ_{ex}^m is the magnetic part of the Kohn-Sham potential at the site m [evaluated in terms of the LMTO band-center (C) parameters as $\Delta_{\mathrm{ex}}^m = \frac{1}{2}(C_m^{\uparrow} - C_m^{\downarrow})$];[19] Tr_L denotes the trace over the orbital indices, and ε_F is the Fermi energy. This method allows us to calculate magnetic interactions between all possible pairs of atoms (for example, the ones located in Fe and M sublattices), but somewhat sensitive to details of calculations, such as division of the unit cell into atomic spheres and the choice of the LMTO basis.

In the present work, the atomic spheres radii were chosen from the charge neutrality condition inside the spheres so that the total unit-cell volumes were close to the experimental ones (Table I). All calculations have been performed assuming the cubic ($Fm\bar{3}m$) crystal symmetry. The oxygen atoms were placed in the middle between Fe and M unless it is specified otherwise (Sec. V B). The LMTO Hamiltonian was constructed for two separate energy panels. The first one was aimed at describing the low-energy Sr($4p$) and O($2s$) bands; and the second one included the Sr($5sp$,$4d$), Fe($4sp$,$3d$), Mo($5sp$,$4d$), and O($3s$,$2p$) states in the case of Sr_2FeMoO_6 (and similar set of basis orbitals for other compounds).

The main idea of the second approach is to calculate first the Fourier image of magnetic interactions $J_{\mathbf{q}} = \Sigma_m J_m \exp(i\mathbf{q}\mathbf{R}_m)$ ($\mathbf{R}_m$ being the position of the site m) using the spin-spiral LMTO method.[20] For example, for the simple ferromagnet $J_{\mathbf{q}}$ can be found as

$$J_{\mathbf{q}} - J_0 = \left.\frac{\partial^2 E(\mathbf{q},\vartheta)}{\partial \vartheta^2}\right|_{\vartheta=0}, \qquad (3)$$

where $J_0 \equiv J_{\mathbf{q}=0}$ and $E(\mathbf{q},\vartheta)$ is the total energy (in the practical calculations—the one-electron energy, thanks to the local-force theorem[13,16]) corresponding to the spin-spiral configuration with the cone-angle ϑ and the spiral vector $\mathbf{q}$. $J_{\mathbf{q}}$ can be further Fourier transformed to the real-space parameters $\{J_m\}$. This method is less sensitive to details of calculations. However, it is also less flexible. For example, it is rather difficult to extract the interactions between the Fe and M sublattices by using this approach,[21] and if it is not specified otherwise, we will map all the interactions on only one (Fe) sublattice by using the same ϑ for all atoms and by modulating the phases of the spin rotations according to the formula $\mathbf{q}\mathbf{R}_m$ with $\mathbf{R}_m$ running over all the sites, irrespective of the type of sublattices. In this scheme, Fe-M, M-M, etc., interactions are effectively included as the renormalization of (principal) Fe-Fe interactions.

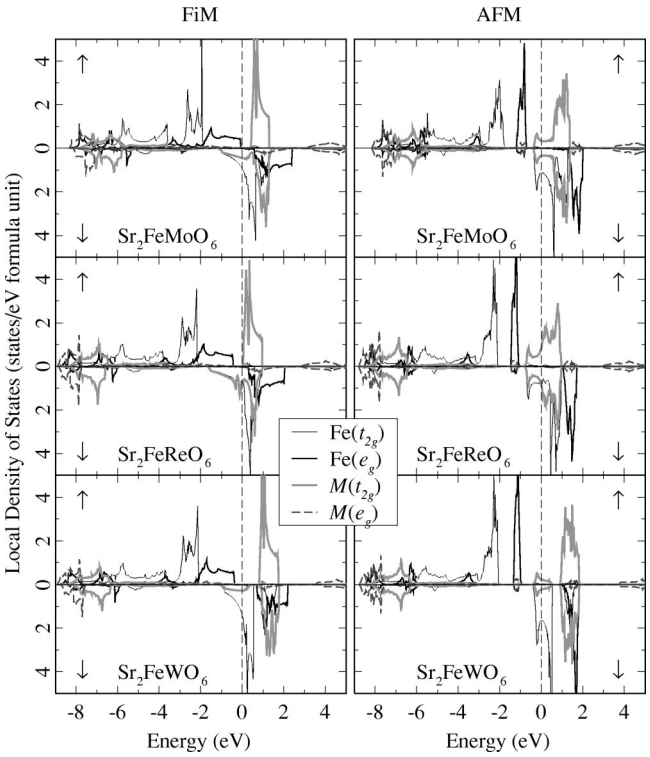

FIG. 1. LSDA density of states for the ferrimagnetic (left) and antiferromagnetic (right) phases of Sr_2FeMO_6 (M = Mo, Re, and W). The Fermi level is at zero.

III. MAIN DETAILS OF ELECTRONIC STRUCTURE AND CHARACTER OF INTERATOMIC MAGNETIC INTERACTIONS

As it was already pointed out before,[2,3,6] the FiM state of Sr_2FeMO_6 (M = Mo, Re, and W) is half metallic (Fig. 1). The Fermi level falls in the gap between the Fe(e_g) and $M(t_{2g})$ bands in the $\uparrow$-spin channel, and crosses a t_{2g} band in the $\downarrow$-spin channel. The composition of this band depends on the material. So, for the Mo and Re compounds, the Fe(t_{2g}) and $M(t_{2g})$ states strongly overlap and equally contribute to the occupied part of the t_{2g} band. In Sr_2FeWO_6, the antibonding W(t_{2g}) states are pushed to the higher-energy region because of stronger hybridization with the O($2p$) states,[6] and only the Fe(t_{2g}) states have significant weight near ε_F. Due to the HM character of the FiM phase, the total spin magnetic moment is integer and is equal to $4\mu_B$ in the case of Sr_2FeMoO_6 and Sr_2FeWO_6, and $3\mu_B$ in the case of Sr_2FeReO_6. The composition and the filling of the t_{2g} band control the magnitude of the spin magnetic moment induced at the M site, which takes the following values (inside atomic spheres): $0.17\mu_B$ (Sr_2FeMoO_6), $0.74\mu_B$ (Sr_2FeReO_6), and $0.06\mu_B$ (Sr_2FeWO_6). Since these moments originate from the filling of the $\downarrow$-spin band, they are antiparallel to the Fe moments, that actually explains the

ferrimagnetic character of this phase.

The main details of the obtained electronic structure are in a good agreement with results of full-potential augmented plane waves[2,3,22] and pseudopotential[6] calculations.

Undoubtedly, the partly occupied t_{2g} band in the HM regime should be the source of ferromagnetism, which have the same origin as the famous double exchange in colossal-magnetoresistive manganites,[23] and may be modified by the fact that a similar mechanism operates also between chemically different Fe and *M* sites in the case of DP.[7]

However, is this the only one interaction, which determines the magnetic behavior of the DP? Unfortunately, the situation is more complicated. As we shall see in the next section, the partly occupied t_{2g} band gives rise not only to the FM double exchange, but also to a nonvanishing AFM superexchange (SE) interaction, the existence of which is related to the fact that the exchange splitting Δ_{ex}^{Fe} is finite.[23]

Less attention in the literature is paid to another fact: in the DP the fully polarized Fe(e_g) states are *half filled*, that gives rise to the *antiferromagnetic superexchange* mechanism associated with the e_g *electrons*. The SE interactions are mediated by quite long Fe-O-*M*-O-Fe paths and therefore expected to be not particularly strong. However, such an intuitive picture can be rather misleading. A rough idea about the strength of the e_g superexchange can be obtained from the analysis of the density of states (Fig. 1): by going from the FM to the type-II AFM phase, the Fe(e_g) band shrinks very significantly, from 2.0 to 0.5 eV, similar to the canonical rock-salt transition-metal monoxides.[24] Therefore, the interaction between e_g orbitals of neighboring Fe atoms remains strong even in the double perovskite structure.

One can also exploit some analogy with manganites. In the latter, the FM ordering is stabilized by the double exchange (DE) mechanism associated with the e_g electrons, which is much stronger than the AFM SE interactions between the t_{2g} electrons.[25] Then, at least very naively in the DP, one could expect the opposite trend: a relatively week FM t_{2g} double exchange competing with a strong AFM e_g superexchange.

Thus, from this very simplified analysis of the electronic structure one may expect that the stability of the FiM phase in the DP is by no means a trivial problem: there are several different mechanisms favoring both FM and AFM spin alignments, and it is not *a priori* clear that the FM interactions will prevail.

IV. MAGNETIC INTERACTIONS IN THE FERRIMAGNETIC STATE: LSDA FOR IDEAL DOUBLE PEROVSKITES

Qualitative discussions in the preceding section are supported by direct calculations of magnetic interactions (3) in the FiM state (Fig. 2). Since $J_0 - J_{\mathbf{q}}$ is nothing but the second derivative of the total energy, the negative value of the parameter $J_0 - J_{\mathbf{q}}$ indicates that the FiM state is unstable with respect to a noncollinear spin-spiral ordering with the vector $\mathbf{q}$. $\mathbf{q}=(\pi/a_0)[0,1,0]$ and $\mathbf{q}=(\pi/2a_0)[1,1,1]$ (a_0 being the cubic perovskite lattice parameter equal to the nearest Fe-*M* distance in the double perovskite structure) corresponds to the type-I and type-II AFM ordering, respectively. Thus, for all considered compounds the FiM state appears to be unstable.

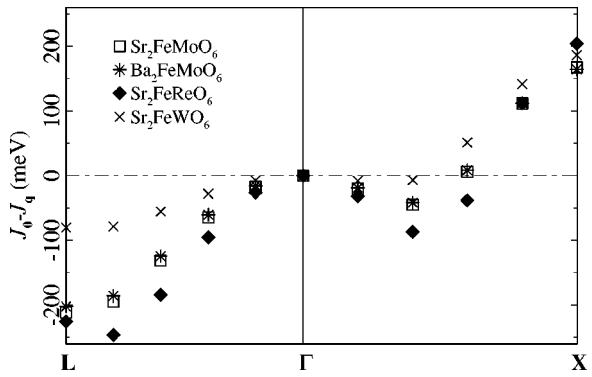

FIG. 2. Behavior of magnetic interactions in the reciprocal space (spin-spiral calculations near the ferrimagnetic state). $\mathbf{L}=(\pi/2a_0)[1,1,1]$, $\mathbf{\Gamma}=[0,0,0]$, and $\mathbf{X}=(\pi/a_0)[0,1,0]$ are the high-symmetry points of the face-centered-cubic Brillouin zone; a_0 is the nearest Fe-*M* distance (the lattice parameter of the cubic perovskite structure).

A more clear picture can be obtained by transforming $J_{\mathbf{q}}$ into the real space. For these purposes we adopt the following notations in the Fe sublattice: $J_1^{\text{Fe-Fe}}$ will stand for the nearest-neighbor (nn) interactions between sites separated by the vector $[a_0,a_0,0]$, and $J_2^{\text{Fe-Fe}}$ is the next-nn interactions between sites separated by the vector $[0,0,2a_0]$. These parameters are listed in Table II. Although the nn coupling $J_1^{\text{Fe-Fe}}$ is ferromagnetic, it is considerably weaker than the next-nn AFM interaction $J_2^{\text{Fe-Fe}}$, which makes the whole FiM structure unstable. Note that in terms of these two interactions, the FiM ordering will be stable if $J_1^{\text{Fe-Fe}} > |J_2^{\text{Fe-Fe}}|$.

The double exchange (J^D) and superexchange (J^S) contributions to $J_1^{\text{Fe-Fe}}$ can be estimated very roughly by assuming that both mechanisms can be described in terms of a universal effective nn transfer integral (t) in the Fe sublattice, and employing the fact that J^D and J^S should be proportional to t and t^2, respectively. Then, by varying the lattice parameters in the interval $0.99 \leqslant a/a_0 \leqslant 1.01$, adopting the formula:[17,18]

$$J_1^{\text{Fe-Fe}}(a) = J^D \frac{t(a)}{t(a_0)} + J^S \frac{t^2(a)}{t^2(a_0)},$$

and assuming the canonical scaling for the transfer integral: $t(a) \propto a^{-\alpha}$, one can obtain the following parameters, in the case of Sr_2FeMoO_6: $J^D = 18.3$ meV, $J^S = -9.0$ meV, and

TABLE II. Magnetic interactions in the ferrimagnetic state obtained in the spin-spiral calculations.

Compound	$J_1^{\text{Fe-Fe}}$ (meV)	$J_2^{\text{Fe-Fe}}$ (meV)
Sr_2FeMoO_6	9.3	−26.9
Ba_2FeMoO_6	9.1	−25.9
Sr_2FeReO_6	10.4	−29.6
Sr_2FeWO_6	11.0	−17.8

TABLE III. Magnetic interactions in the ferrimagnetic state obtained in the Green function calculations.

Compound	$J_1^{\text{Fe-Fe}}$ (meV)	$J_2^{\text{Fe-Fe}}$ (meV)	$J_1^{\text{Fe-Mo}}$ (meV)
Sr_2FeMoO_6	6.2	−21.5	−1.21
Sr_2FeReO_6	4.5	−27.9	−11.6

$\alpha = -8.16$. It is interesting to note that even J^D alone appears to be too small to overcome $J_2^{\text{Fe-Fe}}$ and stabilize the FiM phase. The AFM counterpart J^S makes the situation even worse.

In order to check consistency of our analysis, we calculated the same parameters by using the Green function technique (2). They are listed in Table III for Sr_2FeMoO_6 and Sr_2FeReO_6. For $J_1^{\text{Fe-Fe}}$ and $J_2^{\text{Fe-Fe}}$ there is a reasonable agreement with results of the spin-spiral calculations (Table II), especially by taking into account very different treatment of the intersublattice magnetic interactions in these two approaches. The nn interaction $J_1^{\text{Fe-}M}$ between Fe and M sites separated by the vector $[a_0,0,0]$ is also shown in Table III. This interaction is antiferromagnetic, that additionally stabilizes the FiM ordering,[4,5,7] and readily explains the fact that $J_1^{\text{Fe-Fe}}$ is typically larger in the spin-spiral approach, where the contributions associated with $J_1^{\text{Fe-}M}$ are effectively included in the renormalization of magnetic interactions in the Fe sublattice.

$J_1^{\text{Fe-}M}$ appears to be small in Sr_2FeMoO_6. The additional magnetic polarization of the $M(t_{2g})$ states in the case of Sr_2FeReO_6 enhances $J_1^{\text{Fe-}M}$. However, this enhancement is not particularly strong and cannot explain the local stability of the FiM phase. For example, by taking into account all three interactions $J_1^{\text{Fe-}M}$, $J_1^{\text{Fe-Fe}}$, and $J_2^{\text{Fe-Fe}}$, it is easy to show that the FiM phase will be *unstable* with respect to a spin-spiral ordering with $\mathbf{q} \| [1,1,1]$ if

$$2(J_1^{\text{Fe-Fe}} + J_2^{\text{Fe-Fe}}) - J_1^{\text{Fe-}M} < 0. \tag{4}$$

This inequality is satisfied for the parameters listed in Table III. As we will see in Sec. V A, $J_1^{\text{Fe-}M}$ can be further enhanced by the Coulomb repulsion ΔU at the Fe sites, which is presumably missing in the LSDA approach. However, even for relatively large ΔU the inequality (4) will be largely intact, and the FiM ordering will be unstable. Thus, contrary to recent suggestions,[4,5,7] we found that the interaction $J_1^{\text{Fe-}M}$, though can play some role in the problem, fails to explain not only high T_C but also the local stability of the FiM ordering in the DP if it is considered in combination with other magnetic interactions in the Fe sublattice. Note also that $J_1^{\text{Fe-}M}$ depends on the magnitude of spin magnetization at the M sites. However, this magnetization is only *induced by the hybridization* with the Fe states and the situation is cardinally different from the behavior of localized magnetic moments (at least at the level of LSDA). In such a case $J_1^{\text{Fe-}M}$ depends on the magnetic state in which it is calculated. In the Fe-spin-disordered paramagnetic phase, as well as in the AFM phase, the M moment is zero. Hence, $J_1^{\text{Fe-}M}$ should be also zero. Therefore, the behavior of magnetic interaction near T_C should be very different, and the parameter $J_1^{\text{Fe-}M}$ evaluated in the fully spin-polarized FiM state cannot be applied to the analysis of the magnetic transition temperature.

TABLE IV. Magnetic interactions in the type-II antiferromagnetic state obtained in the spin-spiral calculations. Two values of the parameter $J_1^{\text{Fe-Fe}}$ correspond to interactions between nearest-neighbor Fe sites with the same (the first number) and opposite (the second number) spins in the type-II antiferromagnetic structure.

Compound	$J_1^{\text{Fe-Fe}}$ (meV)	$J_2^{\text{Fe-Fe}}$ (meV)
Sr_2FeMoO_6	16.4, 18.6	−15.2
Sr_2FeWO_6	17.4, 21.3	−13.5

Finally, parameters $J_1^{\text{Fe-Fe}}$ and $J_2^{\text{Fe-Fe}}$ can be extracted (at least formally) by mapping the total energies of the FiM, type-I and type-II AFM states onto the Heisenberg model. Using results of GGA calculations for Sr_2FeWO_6 reported in Ref. 6 we find $J_1^{\text{Fe-Fe}} = 18.1$ meV and $J_2^{\text{Fe-Fe}} = -7.5$ meV. Similar to the analysis of the local stability of the FiM phase, the nn coupling appears to be ferromagnetic, while the next-nn coupling antiferromagnetic. However, according to the total energy calculations, $J_1^{\text{Fe-Fe}}$ is stronger than $J_2^{\text{Fe-Fe}}$. This apparent disagreement with the conclusion based on the local stability arguments should not be taken as a surprise, because formally these two techniques bring the information about very different quantities (see also discussions in Sec. II). In the total energy calculations, the inequality $J_1^{\text{Fe-Fe}} > |J_2^{\text{Fe-Fe}}|$ simply means that the FiM state has lower energy, and this statement is simply paraphrased onto the language of Heisenberg model. Formally, these parameters have no other physical meaning and cannot be applied to the analysis of the local stability of neither the FiM nor the AFM state. On the other hand, the local stability implies the knowledge of second derivative of the total energy, which cannot be directly converted to the total energy itself. Thus, these are simply two *complementary* pieces of information.

By combining results of total energy calculations[6] with the local stability arguments, one may conclude that although the FiM state has the lowest energy amongst the collinear magnetic configurations, it is not a local minimum of the total energy. Probably, the true magnetic ground state of the ordered DP in LSDA and GGA, will be a noncollinear spin-spiral state with $\mathbf{q} \| [1,1,1]$. This is qualitatively supported also by calculations of the inter-atomic magnetic interactions in the type-II AFM state (Table IV). We note the following: in the FiM state we had the inequality $J_1^{\text{Fe-Fe}} < |J_2^{\text{Fe-Fe}}|$, meaning that this state was unstable (with respect to the type-II AFM ordering). However, in the type-II AFM state we obtain the opposite inequality $J_1^{\text{Fe-Fe}} > |J_2^{\text{Fe-Fe}}|$,[26] meaning that this state is also unstable (but already with respect to the FiM ordering). Therefore, the real magnetic ground state of the DP should be in between the FiM and type-II AFM states. Presumably, that is the situation realized in Sr_2FeWO_6 (we will return to this problem again in Sec. VII).

V. WHAT MAKES THE FERRIMAGNETIC PHASE STABLE?

A. Choice of exchange-correlation potential and Coulomb interactions beyond LSDA

As we have seen in the previous section, the FiM state in the ordered DP is unstable in the LSDA. The first serious question we have to address is how reliable is this picture, because the LSDA description is not perfect, especially for the strongly correlated systems.[27] At the present state we do not really know how serious is this problem for the DP and whether one should concentrate on the improvement of the LSDA description (that is still an unresolved problem, despite numerous efforts in this direction—see, e.g., Ref. 27) or try to find a new physical mechanism (apart from the correlations) that would explain appearance of the ferromagnetism in these compounds. In this section, we try to estimate possible roles played by Coulomb correlations in stability of the FiM ordering, using Sr_2FeMoO_6 as an example.

First, there are some possibilities to shift the balance between the FM and AFM interactions in Sr_2FeMoO_6 by simply choosing different exchange-correlation potentials in (or around) the LSDA.[28] The general strategy should be to increase Δ_{ex}^{Fe}. Then, according to the model tight-binding analysis,[23] one could expect that larger Δ_{ex}^{Fe} will suppress the AFM SE interactions (which are proportional to $1/\Delta_{ex}$), while the FM double exchange should not be affected by Δ_{ex}^{Fe}, unless it changes the Fe-M hybridization in the metallic $\downarrow$-spin channel. Along this line, the GGA approach[29] does not give any improvement, at least if it is implemented in the atomic spheres approximation: for example, spin-spiral calculations yield the following values of the parameters: $J_1^{Fe\text{-}Fe}=9.1$ meV and $J_2^{Fe\text{-}Fe}=-30.9$ meV (i.e., the situation appears to be even worse rather than in LSDA—see Table II).

Another approach along this line is somewhat hypothetical. It is well known that correlations in LSDA suppress Δ_{ex}.[30] Therefore, by taking into account only the exchange part of the LSDA potential we can get an upper estimate for Δ_{ex}^{Fe} on the level of LSDA. The corresponding density of states is shown in Fig. 3. One can clearly see that the splitting between the $\uparrow$- and $\downarrow$-spin Fe($3d$) states is significantly increased. This causes some redistribution in the occupied part of the spectrum, whereas the states located near ε_F, and especially the position of the $\downarrow$-spin Fe(t_{2g}) and Mo(t_{2g}) bands, are practically unchanged. These changes of the electronic structure will tend to stabilize of the FiM ordering. However, the effect is not sufficiently strong and $J_0-J_{\mathbf{q}}$ remains negative along the **Γ-L** direction in the reciprocal space (Fig. 4). Corresponding parameters of the magnetic interactions, after transformation to the real space, are $J_1^{Fe\text{-}Fe}=10.7$ meV and $J_2^{Fe\text{-}Fe}=-12.7$ meV.

Another possible correction of the electronic structure which we want to investigate is in the spirit of the LDA $+U$ approach.[31] At the first sight the idea appears to be simple and what one has to do is to correct the form and the magnitude of the on-site Coulomb interactions for the ''localized'' states. The first candidates for this correction are the

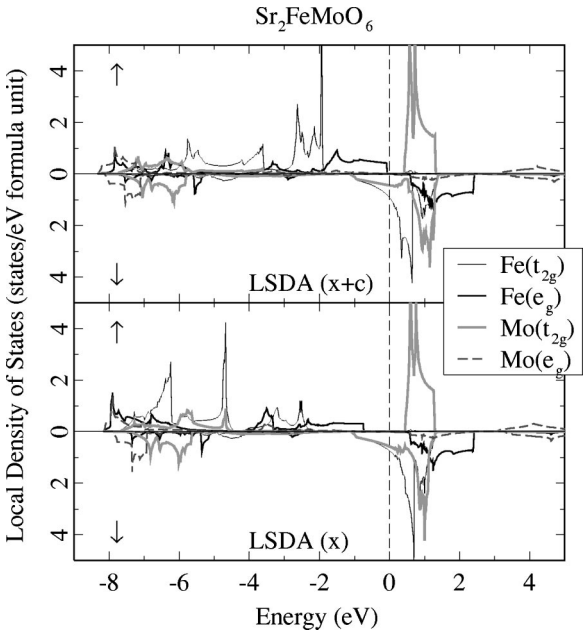

FIG. 3. LSDA density of states for the ferrimagnetic phase of Sr_2FeMoO_6 calculated using both exchange and correlation parts of the potential (x+c), and the exchange part only (x). The Fermi level is at zero.

Fe($3d$) states. However, the progress along this line is hampered by the fact that already for the transition-metal monoxides all important parameters controlling the electronic properties, such as the magnitude of the on-site Coulomb repulsion U and the charge-transfer energy,[32] are not well defined in the framework of LDA$+U$.[16] The problem is even more serious for the DP where there is the additional group of $M(t_{2g})$ states, which may have strong influence on the physical properties, but the position of which with respect to the Fe($3d$) and O($2p$) states is absolutely uncontrollable at the level of LDA$+U$. Therefore, we take an empirical approach that is based on our previous analysis of spectroscopic and magnetic properties of MnO (Ref. 16) and $LaFeO_3$ (Ref. 33). We have found that for compounds that have common $3d_{\uparrow}^5 3d_{\downarrow}^0$ configuration of the transition-metal

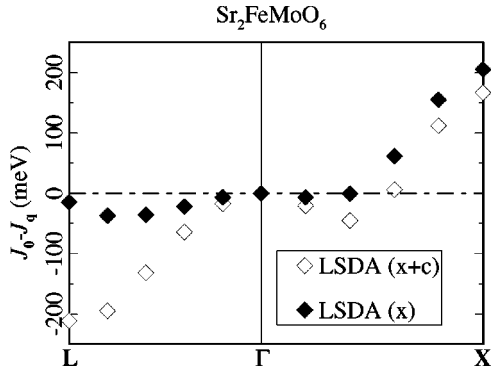

FIG. 4. Behavior of magnetic interactions in the reciprocal space for two types of exchange-correlation potential in LSDA, which include both exchange and correlation parts (x+c), and the exchange part only (x).

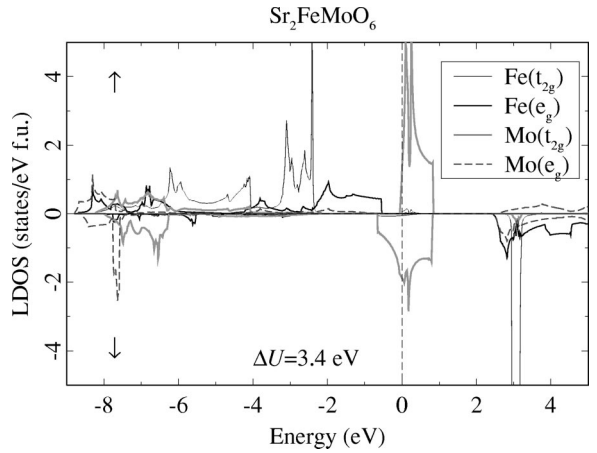

FIG. 5. Density of states obtained after shifting the minority-spin Fe($3d$) states up by 3.4 eV. The Fermi level is at zero.

sites, a good improvement of the LSDA description could be obtained by increasing the intra-atomic exchange splitting and shifting the unoccupied $\downarrow$-spin $3d$ states up by ΔU. The adjustable parameter ΔU could be fixed by fitting the optical or photoemission spectra. For example, in $LaFeO_3$ the shift of unoccupied states by $\Delta U \sim 2$ eV gave a good description for the local magnetic moments, optical and photoemission data.[33,34]

The same strategy seems to be reasonable for the Fe($3d$) states in Sr_2FeMoO_6, which are also close to the half filling. The low-energy optical absorption observed around 0.5 eV is typically ascribed to the ''charge transfer'' excitations from Fe(e_g) to Mo(t_{2g}) band in the $\uparrow$-spin channel,[4,35] and impose a strong constraint on the position of occupied Fe(e_g) states. Therefore, the relative position of the Fe(e_g) to Mo(t_{2g}) bands is rigidly fixed and the only possible degree of freedom for the ΔU operator is the shift of unoccupied $\downarrow$-spin states (see also the discussions of optical conductivity in Sec. VI).

A typical example of the density of states after such shift is shown in Fig. 5. It strongly resembles the picture discussed recently by Kanamori and Terakura.[7] As the $\downarrow$-spin Fe($3d$) states are moved to the higher-energy region, the population of Mo(t_{2g}) states increases. Therefore, the local magnetic moment at Mo sites will also increase. It additionally stabilizes the nn AFM interaction $J_1^{\text{Fe-Mo}}$ between Fe and Mo (Fig. 6), in agreement with arguments presented in Ref. 7. Note also that the electronic structure shown in Fig. 5 is (nearly) half-metallic, and the main contribution near ε_F comes from the Mo(t_{2g}) states. Hence, the Mo moment is already close to the saturated value of $1\mu_B$. In such a situation, an additional Coulomb interaction U_M on the Mo sites can increase the splitting between the $\uparrow$- and $\downarrow$-spin Mo(t_{2g}) states, but without changing the Mo moment and $J_1^{\text{Fe-Mo}}$. Therefore, we do not expect that a small U_M parameter may alter our conclusions.[36] This is qualitatively supported by results of LDA$+U$ calculations including the Coulomb U both on the Fe and Mo sites.[22]

How will the change of $J_1^{\text{Fe-Mo}}$ affect the local stability problem of the FiM state, if considered in combination with

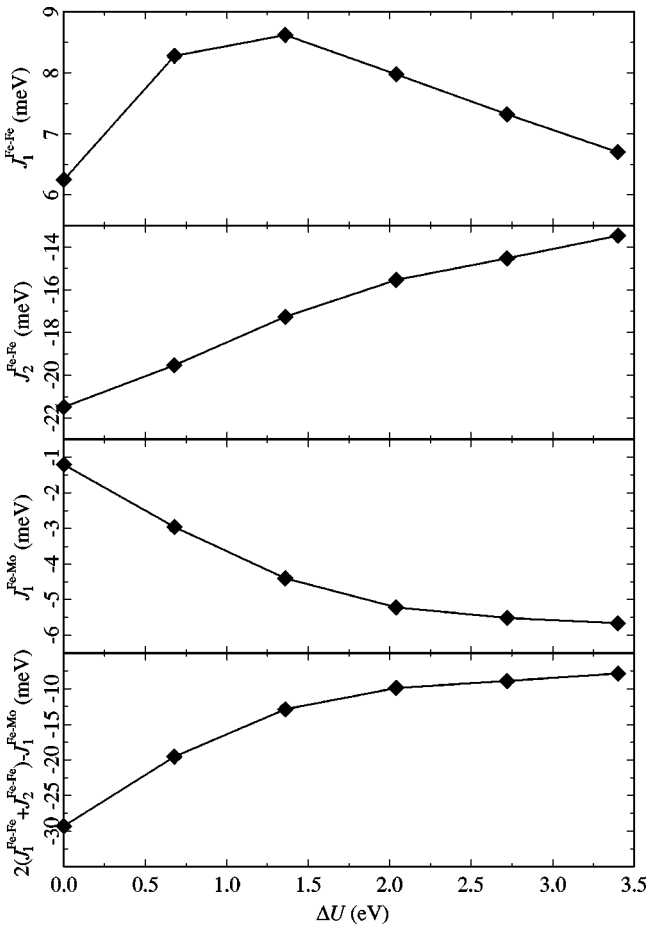

FIG. 6. Magnetic interactions in Sr_2FeMoO_6 after additional shift of the minority-spin Fe($3d$) states by ΔU (from the Green function calculations).

other magnetic interactions in the Fe sublattice? First, ΔU suppresses the AFM SE interactions in the system and thereby substantially reduces $J_2^{\text{Fe-Fe}}$. This favors the FiM alignment. The behavior of $J_1^{\text{Fe-Fe}}$ is more complicated. On the one hand, ΔU suppresses the AFM SE contributions also to $J_1^{\text{Fe-Fe}}$, which explains the increase of $J_1^{\text{Fe-Fe}}$ for small ΔU. On the other hand, ΔU increases the energy splitting between the Fe(t_{2g}) and Mo(t_{2g}) states, and suppresses all kinetic hoppings between Fe(t_{2g}) orbitals operating via the Mo(t_{2g}) states in the $\downarrow$-spin channel. In addition, ΔU depopulates the Fe(t_{2g}) states. These two mechanisms will gradually destroy the FM DE interaction operating between the Fe(t_{2g}) orbitals. They dominate in the region of larger ΔU, where $J_1^{\text{Fe-Fe}}$ decreases.

Taking into account three interactions $J_1^{\text{Fe-Mo}}$, $J_1^{\text{Fe-Fe}}$, and $J_2^{\text{Fe-Fe}}$, we evaluated the stability condition of the FiM phase with respect to the spin-spiral ordering given by Eq. (4), the left-hand side of which is also shown in Fig. 6. For all values of ΔU we have considered, the inequality (4) is satisfied, meaning that the FiM ordering remains *unstable*. Moreover, the left-hand side of this inequality becomes saturated for large ΔU, and an additional increase of the on-site Coulomb repulsion will hardly change our conclusion.

Thus, the Coulomb correlations beyond LSDA, though may play some role in the problem, will hardly explain alone the local stability of the FiM phase in DP. Therefore, in the next few sections we consider several other scenarios, which are not directly related to Coulomb correlations.

B. Breathing distortion

Due to the size and chemical differences between the Fe and *M* atoms, the double perovskite structure is subjected to the breathing distortions of alternating FeO_6 and MO_6 octahedra. The experimental situation about the direction and the magnitude of this distortion in Sr_2FeMoO_6 is rather controversial. The first x-ray diffraction measurements performed on a single crystal of Sr_2FeMoO_6 indicated some contraction of the MoO_6 octahedra, but the effect was found to be small: in terms of the Fe-O and Mo-O bond lengths, the experimental distortion was characterized by the ratios $d_{\text{Fe-O}}/d_{\text{Fe-Mo}}=0.499$ and 0.509, correspondingly in the *x*-*y* plane and along the *z* direction of the tetragonal $I4/mmm$ phase.[4] Very similar distortion, $d_{\text{Fe-O}}/d_{\text{Fe-Mo}}=0.507$ was reported for the cubic $Fm\bar{3}m$ phase of Sr_2FeMoO_6.[35] This trend was, however, disputed in the subsequent publication,[22] where the opposite direction and much larger magnitude of the oxygen displacement have been suggested: $d_{\text{Fe-O}}/d_{\text{Fe-Mo}}=0.488$ and 0.477, correspondingly in the *x*-*y* plane and along the *z* direction of the tetragonal $I4/mmm$ sample. However, the next report suggested the lower ($I4/m$) symmetry of Sr_2FeMoO_6 with $d_{\text{Fe-O}}/d_{\text{Fe-Mo}}=0.506$ (the *x*-*y* plane) and 0.503 (the *z* direction).[37]

The situation seems to be clearer in Sr_2FeReO_6 and Sr_2FeWO_6. Due to the large size of Re and W atoms, the oxygen moves in the direction of Fe. The magnitude of the oxygen displacement in Sr_2FeReO_6 can be estimated as $d_{\text{Fe-O}}/d_{\text{Fe-Re}}\simeq 0.49$.[12]

In this section we discuss the effects of breathing distortion on the magnetic interactions in the cubic $Fm\bar{3}m$ structure. As in the previous section we take Sr_2FeMoO_6 as an example.

Results of calculations are summarized in Fig. 7. The situation is very intriguing, because the oxygen displacement from the midpoint position in *both directions* tends to stabilize the FiM ordering. Although the microscopic mechanism of this behavior is very different for two different directions, in both cases it is related to the fact that the Fe($3d$) and Mo($4d$) states form *antibonding* bands after the hybridization with the O($2p$) states. Therefore, the oxygen displacement towards Fe will result in an upward shift of the Fe($3d$) bands and a downward shift of the Mo($4d$) bands, and vice versa for the opposite direction of the lattice distortion.

The upward shift of the Mo($4d$) band in the regime $d_{\text{Fe-O}}/d_{\text{Fe-Mo}}>0.5$ will affect the SE interactions operating via the Mo($4d$) states. In this case the energy gap between the Fe($3d$) and Mo($4d$) states will play the same role as the charge-transfer energy in the conventional transition-metal monoxides. The increase of the gap will suppress the SE interactions.[38] However, in the LSDA this change is not sufficient to alter the inequality $J_0-J_{\mathbf{q}}<0$ and stabilize the FiM ordering, even for relatively large distortion $d_{\text{Fe-O}}/d_{\text{Fe-Mo}}=0.525$ (see Fig. 7).

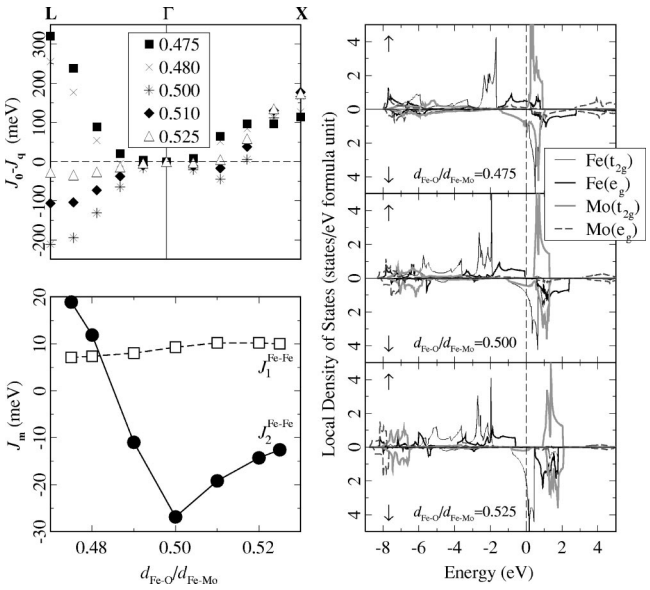

FIG. 7. Breathing distortion in Sr_2FeMoO_6. Left panel: magnetic interactions in the reciprocal space as a function of breathing distortion $d_{\text{Fe-O}}/d_{\text{Fe-Mo}}$ (the ratio of Fe-O and Fe-Mo bond lengths), and results of their Fourier transformation to the real-space parameters $J_1^{\text{Fe-Fe}}$ and $J_2^{\text{Fe-Fe}}$. Right panel: examples of density of states for several $d_{\text{Fe-O}}/d_{\text{Fe-Mo}}$ ratios. The Fermi level is at zero.

Another direction of the breathing distortion $d_{\text{Fe-O}}/d_{\text{Fe-Mo}}<0.5$ seems to be more promising. However, the stabilization of the FiM ordering in this regime is directly related to demolishing of the HM character of electronic structure of Sr_2FeMoO_6. Particularly, for $d_{\text{Fe-O}}/d_{\text{Fe-Mo}}\leqslant 0.49$ the Fermi level crosses the ↑-spin Fe(e_g) band and the distortion activates an additional double exchange mechanism associated with the e_g electrons, like in the perovskite manganese oxides.[18] This DE interaction is very strong so that the coupling $J_2^{\text{Fe-Fe}}$ can even become ferromagnetic. Of course, in such a situation the FiM ordering can be easily stabilized. This scenario is accompanied by a sharp decrease in the saturation moment, up to $2.8\mu_B$ per formula unit for $d_{\text{Fe-O}}/d_{\text{Fe-Mo}}=0.475$.

At the present stage, it is not clear up to which extent this mechanism can operate in realistic compounds. According to the experimental data,[4,12,35,37] the large oxygen displacement towards the Fe atoms seems to be unlikely in Sr_2FeMoO_6, but may take place in Sr_2FeReO_6. Since the weight of the W($5d$) states near ε_F is small in Sr_2FeWO_6, the breathing distortion (of a reasonable magnitude) will cause only a rigid shift of the Fe(t_{2g}) and Fe(e_g) bands, without changing their population. Therefore, it should not affect the magnetic ground state of Sr_2FeWO_6.

C. Antisite defects: Supercell calculations

One of the very important factors that affect the magnetic behavior of DP is the presence of antisite defects. Typically,

the total concentration of the Fe and M atoms in Sr_2FeMO_6 is well controlled and is close to 100%. However, it is much more difficult to control the distribution of the Fe and M atoms between two different sublattices. In realistic compounds there is always a certain number of antisite defects, when some of the atoms from the Fe sublattice are interchanged with the same number of atoms from the M sublattice. Typically, the antisite defects are randomly distributed and their number is characterized by the degree of Fe/M ordering of the sample, which can be probed by an x-ray diffraction. This characteristic strongly depends on the compound, and is typically higher for polycrystalline samples where the ordering needs to be established coherently only within smaller-sized grains (in comparison with the whole volume of a single crystal). The worst situation was reported for Sr_2FeMoO_6 single crystal, where due to the proximity of atomic sizes of Fe and Mo, the degree of Fe/Mo ordering is rather low and typically varies from 80% to 92% (at the best).[4,39] In polycrystalline Sr_2FeMoO_6 this characteristic can be improved up to 97%,[8] which is accompanied by a growth of saturation magnetization up to the record $3.7\mu_b$ value (in comparison with $3.2\mu_b$ reported for the single crystal—Ref. 4). In Sr_2FeReO_6, the degree of Fe/Re ordering is about (or may be even higher than) 95%.[12] Sr_2FeWO_6 is believed to be the most ordered compound (almost 100% of the Fe/W ordering, presumably due to the large difference of atomic sizes of Fe and W).[11]

The implication of antisite defects to the magnetic behavior of DP was already discussed in the literature. Particularly, the relatively low saturation moment in Sr_2FeMoO_6 can be easily accounted for in terms of the antisite defects, using both the ionic picture for localized magnetic moments at the Fe and Mo sites,[4] and the itinerant one based on the Friedel arguments.[40]

In this section we will argue that the antisite defects can also be one of important physical ingredients that can lead to stability of the FiM ordering in DP. We begin with the analysis of a hypothetical picture, in which the antisite defects are ordered and can be simulated by means of ordinary supercell calculations. We consider the supercell containing four formula units of Sr_2FeMoO_6 (Fig. 8). The antisite defect was simulated by interchanging one pair of Fe and Mo atoms (denoted as Fe_5 and Mo_2) so to preserve the cubic symmetry of the system. This configuration corresponds to only 75% of the Fe/Mo ordering, which is lower than in the experiment.[4] Nevertheless, such calculations can provide useful information about the *local* redistribution of magnetic interactions around the defect.

Parameters of magnetic interactions, calculated using the Green function technique, are summarized in Table V. We considered two situations: when the spin magnetic moment at the impurity Fe atom (Fe_5 in Fig. 8) is aligned ferromagnetically and antiferromagnetically with respect to the spin magnetization of the host (denoted as ''F state'' and ''A state,'' respectively). Contrary to the previous reports,[41] we found that *both* self-consistent solutions exist, though the calculations were conjugated with some technical difficulties.[42] Irrespective of the type of the magnetic coupling, the antisite defect destroys the HM electronic structure

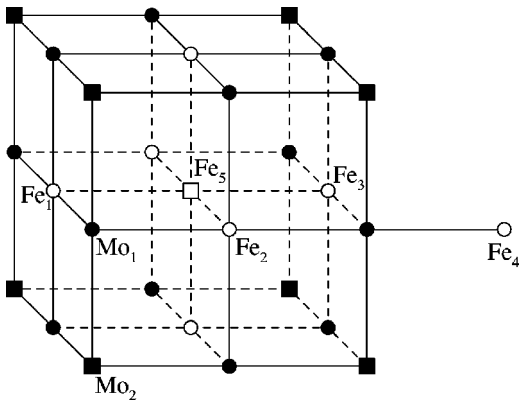

FIG. 8. Positions of the Fe (white symbols) and Mo (black symbols) atoms in the supercell $Sr_8Fe_4Mo_4O_{24}$ used in the calculations of antisite defects. Circles show the atoms that have the same positions as in the ideal double perovskite structure. Squares show the positions of antisite defects obtained after interchanging a single Fe-Mo pair of atoms. Note also the notations of atoms used in the analysis of magnetic interactions in Table V.

(Fig. 9). The spin moment (recalculated per one formula unit) is reduced from $4\mu_B$ in the ordered FiM compound to $3.8\mu_B$ in the F state and $2.4\mu_B$ in the A state. We also note a strong bonding-antibonding splitting of the Mo(t_{2g}) states caused by the hybridization between the impurity and the host. As a result, the $\uparrow$-spin Mo(t_{2g}) states become partially occupied, and the induced Mo moment is polarized *parallel* to the host. Therefore, the theories relying on the strong AFM coupling between the Fe and Mo sites[5,7] become irrelevant near the antisite defects.

According to the nn interactions of the impurity atom with the host (the pair Fe_1-Fe_5), both configurations can be locally stable. In the case of FM alignment (F state), the $\downarrow$-spin Fe(t_{2g}) states of the host and impurity atoms form a broad band, which is partly occupied (Fig. 9). It gives rise to the DE interaction, which explains the FM character of the coupling $J^{Fe_1\text{-}Fe_5}$. The AFM interaction $J^{Fe_1\text{-}Fe_3}$ via the impurity Fe_5 site can be easily understood in terms of the $1/\Delta_{ex}^{Fe}$ expansion in Eq. (2) for the less than half-filled $\downarrow$-spin Fe(t_{2g}) band.[23] However, this behavior may also be an artifact of our model because for the particular supercell geometry shown in Fig. 8, the FM alignment of the Fe_5 spins will automatically lead to the formation of infinite FM chains

TABLE V. Magnetic interactions around antisite defects in Sr_2FeMoO_6 (in meV, see Fig. 8 for notations). The spin magnetic moment at the impurity site Fe_5 can be either parallel (F states) or antiparallel (A states) to the spin magnetization of the host.

Pair	F state	A state
Fe_1-Fe_5	50.6	−40.2
Fe_1-Fe_3	−20.7	1.2
Fe_1-Fe_2	0.6	−0.3
Fe_2-Fe_4	−12.2	−13.4
Fe_1-Mo_1	0	0
Fe_1-Mo_2	−1.1	−1.1

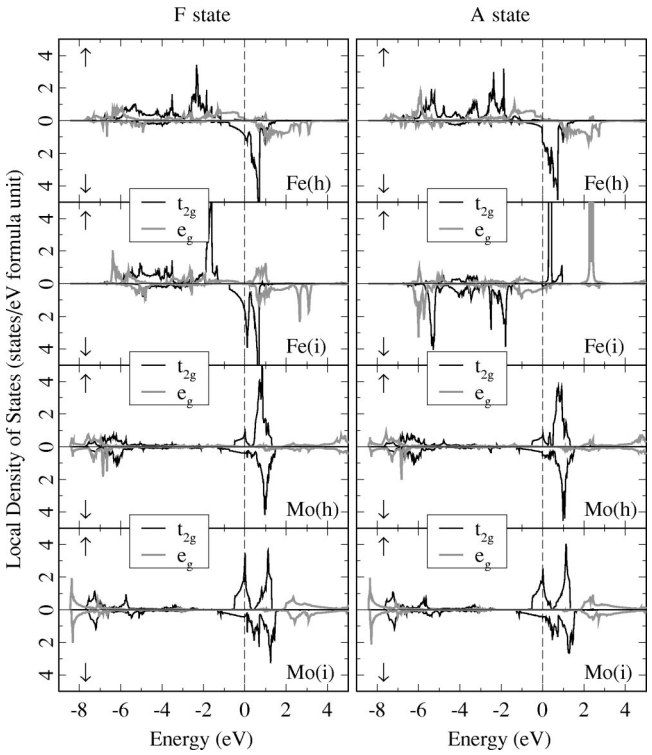

FIG. 9. LSDA density of states for the $Sr_8Fe_4Mo_4O_{24}$ supercell including the antisite defect (shown in Fig. 8). Atoms at the ideal (host) and impurity positions are denoted correspondingly by "h" and "i."

. . . -Fe_1-Fe_5-Fe_3- . . . , which do not exist in realistic disordered samples. Therefore, the itinerant character of the Fe(t_{2g}) states, and the large magnitude of interactions $J^{\mathrm{Fe_1\text{-}Fe_5}}$ and $J^{\mathrm{Fe_1\text{-}Fe_3}}$ can be exaggerated in our model. Moreover, the Coulomb correlations may also play some role in the problem as it can change the character of occupied states near ε_F. For example, according to the scenario considered in Sec. V A, the on-site Coulomb repulsion will move the $\downarrow$-spin Fe(t_{2g}) states away from ε_F and eventually destroy the FM DE coupling. Taking into account these arguments, the formation of the FM spin structure around the impurity Fe sites seems to be rather unlikely.

In the case of AFM alignment (A states), the $3d$ states of the impurity Fe are strongly localized so that their formal electron configuration becomes close to $3d^5_{\uparrow}3d^0_{\downarrow}$ (Fig. 9). This fact readily explains the AFM (superexchange) character of the coupling in the pair Fe_1-Fe_5 (Table V) and the local stability of the state A. Other interactions $J^{\mathrm{Fe_1\text{-}Mo_1}}$, $J^{\mathrm{Fe_1\text{-}Fe_2}}$, and $J^{\mathrm{Fe_2\text{-}Fe_4}}$ involving the host atoms (and corresponding to $J_1^{\mathrm{Fe\text{-}Mo}}$, $J_1^{\mathrm{Fe\text{-}Fe}}$, and $J_2^{\mathrm{Fe\text{-}Fe}}$ in the notations of Sec. IV) are significantly reduced.

Thus, the spin magnetic moments in the Fe sublattice located in the nearest neighborhood to the impurity Fe sites become strongly polarized by the AFM SE interaction with the impurity states. This leads to the formation of ferrimagnetically coupled Fe clusters. Depending on the coupling between the clusters, the FiM spin ordering in DP can be stabilized by the partial antisite disorder. In the next section we will elaborate one such possibility by considering the SE e_g interactions in the disordered sample and argue that this mechanism alone may stabilize the FiM phase in an averaged sense, which is based on the behavior of interatomic magnetic interactions averaged over all possible nearest-neighbor configurations of Fe and Mo atoms.

D. Tight-binding model for the e_g-superexchange interactions modified by the antisite disorder

In the cubic perovskite lattice there is no nn hoppings between the e_g and t_{2g} orbitals.[43] Therefore, we can consider separately the change of the kinetic energy in the system of e_g electrons depending on the magnetic configuration of the Fe and Mo atoms, and their distribution over the sites of the cubic perovskite lattice. Since the Fe(e_g) states in Sr_2FeMoO_6 are simultaneously half filled and fully spin polarized, while the Mo e_g states are unoccupied we may use the standard procedure for calculating the SE interactions, which is to start with the localized atomic limit and include virtual electron hoppings as a perturbation.[44] Namely, by describing the atomic levels as s states (no orbital degeneracy), the zeroth-order Hamiltonian at the site i is given by

$$\hat{H}_i = \Delta_0^i \hat{1} + \frac{\Delta_{\mathrm{ex}}^i}{2} \hat{\boldsymbol{\sigma}} \cdot \mathbf{e}_i , \tag{5}$$

where Δ_0^i is a nonmagnetic "center of gravity," Δ_{ex}^i is the intra-atomic exchange splitting, $\hat{\boldsymbol{\sigma}}$ is the vector of 2×2 Pauli matrices, and $\hat{1}$ is the 2×2 unity matrix. The directions of the spin magnetic moments $\{\mathbf{e}_i\}$ will be specified below.

Then, the energy change at the site i caused by the electron hoppings can be written as

$$\Delta E_i = \sum_j \Delta E_{ij}^{(2)} + \sum_{jkl} \Delta E_{ijkl}^{(4)} ,$$

where

$$\Delta E_{ij}^{(2)} = -\frac{1}{\pi} \mathrm{Im} \int_{-\infty}^{\varepsilon_F} d\varepsilon \, \mathrm{Tr}_S \{ \varepsilon \hat{G}_i(\varepsilon) \hat{t}_{ij} \hat{G}_j(\varepsilon) \hat{t}_{ji} \hat{G}_i(\varepsilon) \} \tag{6}$$

and

$$\Delta E_{ijkl}^{(4)} = -\frac{1}{\pi} \mathrm{Im} \int_{-\infty}^{\varepsilon_F} d\varepsilon \, \mathrm{Tr}_S \{ \varepsilon \hat{G}_i(\varepsilon) \hat{t}_{ij} \hat{G}_j(\varepsilon) \hat{t}_{jk} \hat{G}_k(\varepsilon) \times \hat{t}_{kl} \hat{G}_l(\varepsilon) \hat{t}_{li} \hat{G}_i(\varepsilon) \} \tag{7}$$

correspond to the second and fourth orders of the perturbation theory expansion; $\hat{G}_i$ is the Green function for the Hamiltonian (5); the electron hoppings are restricted by the nearest neighbors and do not depend on spin indices (i.e., $\hat{t}_{ij} \equiv t_{ij}\hat{1}$); and Tr_S denotes the trace over the spin indices.

At this stage we introduce the antisite disorder as follows. We assume that there are two nonequivalent sublattices, A and B (centered at $[0,0,0]$ and $[a_0,a_0,a_0]$, respectively). Let $p_A^{\mathrm{Fe}} \equiv p$ stand for the probability that certain site of the A sublattice is occupied by Fe ($p=1$ correspond to the perfectly ordered sample). Assuming that the distribution of an-

tisite defects is totally random, the remaining probabilities p_A^{Mo}, p_B^{Fe}, and p_B^{Mo} for the stoichiometric Sr_2FeMoO_6 can be obtained from the conditions

$$p_A^{\mathrm{Fe}}+p_A^{\mathrm{Mo}}=1,$$

$$p_B^{\mathrm{Fe}}+p_B^{\mathrm{Mo}}=1,$$

and

$$p_A^{\mathrm{Fe}}+p_B^{\mathrm{Fe}}=1.$$

Then, we take a configurational average of each of $\Delta E_{ij}^{(2)}$ and $\Delta E_{ijkl}^{(4)}$. The procedure can be easily understood by considering the case of $\Delta E_{ij}^{(2)}$ in detail. Since the hoppings are restricted only by the nearest neighbors, it holds $j\in B$ if $i\in A$, and vice versa. Then, one should consider four different combinations depending on whether the sites i and j are occupied by the atoms Fe or Mo. If the distribution of defects is totally random and the individual occupation probabilities of the lattice sites do not correlate with each other, the average of energy change $\overline{\Delta E}_{ij}^{(2)}$ will be given by

$$\begin{aligned}\overline{\Delta E}_{ij}^{(2)}=&p_A^{\mathrm{Fe}}p_B^{\mathrm{Fe}}\Delta E_{ij}^{(2)}(i=\mathrm{Fe};j=\mathrm{Fe})\\&+p_A^{\mathrm{Fe}}p_B^{\mathrm{Mo}}\Delta E_{ij}^{(2)}(i=\mathrm{Fe};j=\mathrm{Mo})\\&+p_A^{\mathrm{Mo}}p_B^{\mathrm{Fe}}\Delta E_{ij}^{(2)}(i=\mathrm{Mo};j=\mathrm{Fe})\\&+p_A^{\mathrm{Mo}}p_B^{\mathrm{Mo}}\Delta E_{ij}^{(2)}(i=\mathrm{Mo};j=\mathrm{Mo}),\end{aligned}$$

where $\Delta E_{ij}^{(2)}(i=\mathrm{Fe};j=\mathrm{Fe})$ means that Eq. (6) should be evaluated by using parameters of electronic structure of Fe both for the i and j sites, etc. The procedure of configurational averaging of $\overline{\Delta E}_{ijkl}^{(4)}$ is a little bit tedious and depends on how many different sites are involved in the path i-j-k-l-i. The prefactor for each contribution $\Delta E_{ijkl}^{(4)}$ is given by the multiplication of the individual probabilities for all *nonequivalent* sites in the path i-j-k-l-i. For example, if all sites are different the prefactor will have the form $p_Ap_Bp_Ap_B$; if $i=k$, $j\neq i$, and $i\in A$ we will obtain the combination $p_Ap_Bp_B$; if $i=k$ and $j=i$ this combination will be reduced to p_Ap_B, etc.

The parameters of the tight-binding model can be chosen as follows. Δ_0^{Fe} and ε_F are taken as the reference point ($\Delta_0^{\mathrm{Fe}}=\varepsilon_F=0$). Then, using the density of states in Fig. 1, Δ_0^{Mo} for the unoccupied e_g states can be estimated as 5.0 eV. The hopping integral $t_{\text{Fe-Mo}}$ can be extracted from the Fe(e_g) bandwidth ($\sim$1.6 eV), assuming that the latter is derived exclusively from the hybridization between the Fe and Mo e_g states separated by Δ_0^{Mo}. Then, in the single-orbital case (i.e., by substituting degenerate e_g levels by a single s state) we obtain $t_{\text{Fe-Mo}}\simeq 0.3$ eV. The remaining nn hoppings $t_{\text{Fe-Fe}}$ and $t_{\text{Mo-Mo}}$ can be estimated by employing the LMTO theory, according to which a hopping $t_{T\text{-}T'}$ is proportional to the square-root of the canonical bandwidths of the states T and T': $t_{T\text{-}T'}\propto(W_TW_{T'})^{1/2}$.[19] Therefore, $t_{\text{Fe-Fe}}$ and $t_{\text{Mo-Mo}}$ can be found by rescaling $t_{\text{Fe-Mo}}$. Using the values $W_{\mathrm{Fe}}\simeq 4.1$ eV and $W_{\mathrm{Mo}}\simeq 7.7$ eV obtained in the LMTO calculations, we find $t_{\text{Fe-Fe}}\simeq 0.2$ eV and $t_{\text{Mo-Mo}}\simeq 0.4$ eV. Finally, the exchange splittings can be estimated from the densities of states (Fig. 1) as $\Delta_{\mathrm{ex}}^{\mathrm{Fe}}=2.6$ eV and $\Delta_{\mathrm{ex}}^{\mathrm{Mo}}=0$.

A good aspect of the configurational averaging employed in this section is that we can treat not only the diagonal disorder caused by the differences of the on-site parameters ($\Delta_0^{\mathrm{Fe}},\Delta_{\mathrm{ex}}^{\mathrm{Fe}}$) and ($\Delta_0^{\mathrm{Mo}},\Delta_{\mathrm{ex}}^{\mathrm{Mo}}$), but also the off-diagonal disorder caused by difference of the interatomic hopping integrals $t_{\text{Fe-Mo}}$, $t_{\text{Fe-Fe}}$, and $t_{\text{Mo-Mo}}$. The off-diagonal disorder typically presents a more challenging problem for theoretical calculations.[45] In this respect, our approach may be even more advanced than the local coherent-potential approximation (CPA).[46–48] Note also, that by the definitions given by Eqs. (6),(7), the SE interactions are short ranged. Therefore, we do not encounter any problems with the self-averaging, known for Ruderman-Kittel-Kasuya-Yosida interactions.[49]

Let us now specify the directions $\{\mathbf{e}_i\}$ of magnetic moments in Eqs. (6) and (7). We closely follow the spin-spiral description employed in Sec. IV and define $\mathbf{e}_i$ as

$$\mathbf{e}_i=(\cos\mathbf{qR}_i\sin\theta_i,\sin\mathbf{qR}_i\sin\theta_i,\cos\theta_i),$$

with $\mathbf{R}_i$ running over both A and B sublattices, and θ_i depending only on the type of sublattice. We consider the case of the AFM alignment of the impurity Fe atoms with respect to the host and invert the direction of exchange field ($\Delta_{\mathrm{ex}}^{\mathrm{Fe}}\rightarrow-\Delta_{\mathrm{ex}}^{\mathrm{Fe}}$) for every Fe occupying the B sublattice. Then, $\theta_A=\theta_B=0$ will correspond to a collinear FiM state of the disordered alloy. For small θ_A and θ_B the total energy change $\overline{\Delta E}=\overline{\Delta E}_A+\overline{\Delta E}_B$ can be written as

$$\begin{aligned}\overline{\Delta E}(\mathbf{q},\theta_A,\theta_B)=&\overline{\Delta E}(\mathbf{q},0,0)+\mathcal{D}_{AA}(\mathbf{q})\theta_A^2+2\mathcal{D}_{AB}(\mathbf{q})\theta_A\theta_B\\&+\mathcal{D}_{BB}(\mathbf{q})\theta_B^2,\end{aligned}$$

and the stability of the FiM state will be determined by the matrix

$$\hat{\mathcal{D}}(\mathbf{q})=\begin{pmatrix}\mathcal{D}_{AA}(\mathbf{q}) & \mathcal{D}_{AB}(\mathbf{q})\\ \mathcal{D}_{AB}(\mathbf{q}) & \mathcal{D}_{BB}(\mathbf{q})\end{pmatrix}. \tag{8}$$

The FiM state will be stable if both the trace (Tr) and the determinant (Det) of $\hat{\mathcal{D}}(\mathbf{q})$ are positive. $\hat{\mathcal{D}}(\mathbf{q})$ can be also Fourier transformed to the effective parameters of magnetic interactions in the real space.

Results of these calculations are shown in Fig. 10 as a function of the antisite disorder p. For $p\geqslant 0.95$, the AFM SE interactions $J_1^{\text{Fe-Fe}}$ and $J_2^{\text{Fe-Fe}}$ operating via the Mo states dominate,[50] and the FiM ordering is unstable (either $\mathrm{Tr}[\hat{\mathcal{D}}]<0$ or $\mathrm{Det}[\hat{\mathcal{D}}]<0$ in Fig. 10). Further increase of the antisite disorder (smaller-p regime) destroys the AFM character of interactions in the A sublattice (and eventually makes the averaged parameters $J_1^{A\text{-}A}$ and $J_2^{A\text{-}A}$ even slightly ferromagnetic). One of the reasons for such behavior is the decrease of the number of Fe-Mo-Fe-Mo-Fe and Mo-Fe-Mo-Fe-Mo paths in the configurational average of $\Delta E_{ijkl}^{(4)}$, which are responsible for the antiferromagnetism. More importantly, the antisite disorder gives rise to the strong AFM SE coupling $J_1^{A\text{-}B}$ between nn sites located in the A and B sublat-

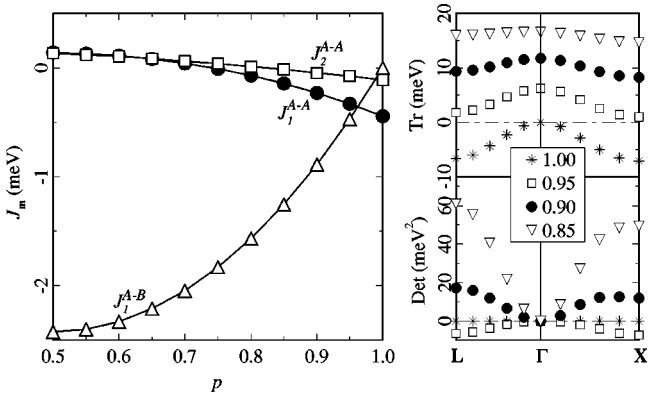

FIG. 10. Effect of the antisite disorder on the superexchange interactions in Sr_2FeMoO_6: results of model tight-binding calculations. Right panel: stability of the ferrimagnetic ordering in the reciprocal space as a function of parameter of the antisite disorder p: the trace and the determinant of the $\hat{\mathcal{D}}$ matrix [Eq. (8)]. Note that the ferrimagnetic ordering is stable if $\mathrm{Tr}[\hat{\mathcal{D}}]>0$ and $\mathrm{Det}[\hat{\mathcal{D}}]>0$. Left panel: parameters of interatomic magnetic interactions obtained after the Fourier transformation of the $\hat{\mathcal{D}}$ matrix to the real space. $p=1$ corresponds to fully ordered sample, where Fe and Mo atoms occupy A and B sublattices, respectively.

tices. The main contribution to $J_1^{A\text{-}B}$ comes from nn interactions in the pairs Fe(host)-Fe(impurity), the number of which increases when p decreases.

Obviously that in the ordered compound ($p=1$) every Fe atom is surrounded only by nonmagnetic Mo atoms and $J_1^{A\text{-}B}=0$. This is actually the main reason why the impurity Fe atoms can stabilize the FiM phase, while the host Mo atoms cannot. Our main point is that the e_g interactions in the cubic perovskite lattice are much stronger than the t_{2g} ones and in the ordered compounds the AFM SE interactions associated with the e_g states easily overcome the (generalized) DE interactions operating in the t_{2g} band, that makes the FiM phase unstable. What we want to do is to force these strong AFM SE interactions between the e_g orbitals to work for the stability of the FiM phase. This can be done by placing an Fe atom on the antisite position. Since the Mo(e_g) states are unoccupied, a similar SE mechanism does not operate between nn Fe and Mo sites. This explains the main difference between the Fe impurities and Mo atoms.

Thus, according to the model analysis, the strong AFM coupling $J_1^{A\text{-}B}$ appears to be sufficient to stabilize the FiM phase if the degree of the antisite disorder in Sr_2FeMoO_6 is $p\leqslant 0.9$. One should take into account that this estimate is based on the analysis of only the SE interactions for the e_g electrons. Presumably, the realistic concentrations p stabilizing the FiM ordering will be even higher because of two reasons. (i) There will be additional AFM SE interactions with the impurity Fe atoms coming from the t_{2g} electrons. (ii) There will be some DE interactions coming from the metallic t_{2g} bands. Note, however, that the second mechanism strongly depends on the mobility of t_{2g} electrons, which will be gradually deteriorated by the antisite disorder.

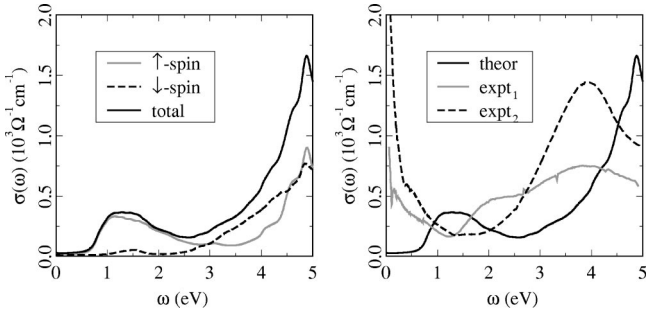

FIG. 11. Optical conductivity for Sr_2FeMoO_6. Left panel: results of LSDA calculations for the hypothetical ferrimagnetic phase—total interband conductivity as well as partial contributions of the ↑- and ↓-spin states. Right panel: the LSDA conductivity in comparison with the experimental data by Y. Moritomo *et al.* ("expt$_1$," measured at $T=300$ K) taken form Ref. 35 and Tomioka *et al.* ("expt$_2$," at $T=10$ K) taken from Ref. 4.

VI. OPTICAL PROPERTIES

In this section we discuss possible implications of various scenarios of the FiM ordering to the form of optical and magneto-optical spectra. As the reference point, we will use results of band-structure calculations for the HM FiM phase of ordered Sr_2FeMoO_6. We would like to emphasize from the very beginning that we treat it as a purely hypothetical example, because in reality this phase is unstable. However, taking into account an enormous popularity of this idealistic picture, we believe that such an analysis can be very useful because it reveals a lot of unresolved problems if compared with the experimental optical data.

For Sr_2FeMoO_6, the experimental optical conductivity spectra were reported in Refs. 4 and 35 (shown in Fig. 11). The optical conductivity is sensitive to the temperature (that presumably explains the difference between the experimental spectra reported in Refs. 4 and 35, and corresponding to 10 K and 300 K, respectively), details of preparation and the quality of sample.[51] Apart from a sharp Drude-like response, both spectra clearly show two structures in the region of interband transitions around 0.5 and 4.0 eV. Using distributions of the LSDA densities of states for the ordered Sr_2FeMoO_6 in the FiM state, they are typically ascribed correspondingly to the Fe(e_g)→Mo(t_{2g}) excitations in the ↑-spin channel and to the O($2p$)→Fe(t_{2g}) charge transfer excitations in the ↓-spin channel.

Although there is a good *qualitative* correspondence between the theoretical calculations and the experimental data, the situation is rather far from the *quantitative* agreement if one takes into account the exact position of the bands and probabilities of the optical transitions. The calculated optical conductivity is shown in Fig. 11.[52] The low-energy part of the spectrum is indeed dominated by the Fe(e_g)→Mo(t_{2g}) excitations in the ↑-spin channel, which are centered around 1.2 eV. The contribution of ↓-spin states to this region is very weak, because of very small probabilities of the interband $t_{2g}\rightarrow t_{2g}$ transitions in the perovskite structure.[53] Another large peak is located around 4.8 eV and caused by the charge transfer excitations from O($2p$) to Mo(t_{2g}) and Fe(t_{2g}) bands simultaneously in the ↑- and ↓-spin channels. Thus,

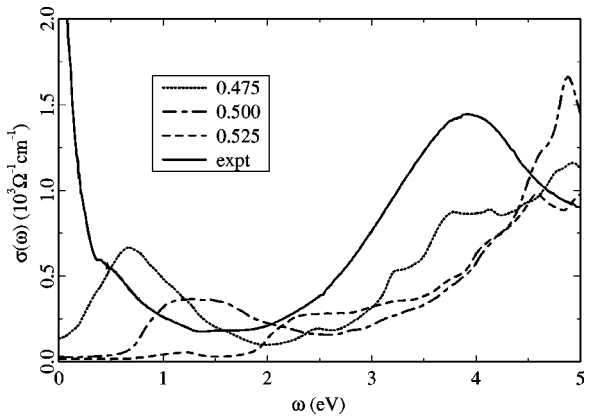

FIG. 12. Effects of breathing distortion on the optical conductivity of Sr_2FeMoO_6: results of LSDA calculations for $d_{\text{Fe-O}}/d_{\text{Fe-Mo}}=0.475$, 0.500, and 0.525 in comparison with the experimental data by Tomioka *et al.* (at $T=10$ K) taken from Ref. 4.

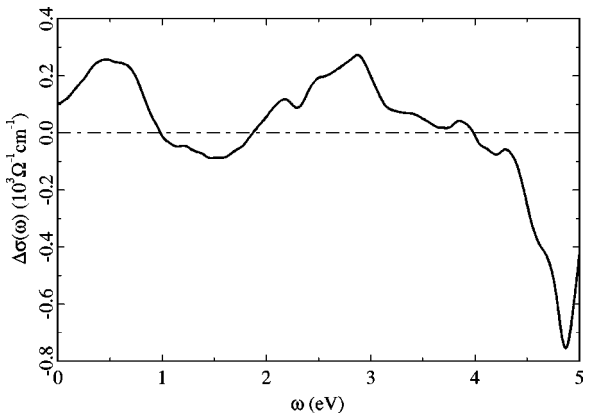

FIG. 13. Contribution of the ''impurity states'' to the optical conductivity of Sr_2FeMoO_6 (the difference between supercell calculations for the state *A* and the ones for the ordered FiM phase).

the theoretical spectrum appears to be shifted with respect to the experimental one by 0.7–0.8 eV towards *higher absorption energies*.

Then, if the Coulomb correlations beyond LSDA indeed play some role in the problem, they should have a rather nontrivial form. For example, the straightforward applications of the Hubbard-*U* correction on the top of the LSDA picture will tend to increase the splitting between the occupied and unoccupied states,[31] and the optical absorption energies (i.e., just the opposite to the experimental trend). Certainly, the situation is not so strict in Sr_2FeMoO_6, where the spectral properties depend not only on *U* but also on the relative position of the Fe($3d$) and Mo($4d$) states. Nevertheless, the experimental optical conductivity imposes severe constraint on the form of this correction. Namely, the distance between the ↑-spin Fe(e_g) and Mo(t_{2g}) bands is rigidly fixed by the position of the first peak of the optical conductivity (being even slightly *smaller* than that in LSDA). Then, it seems that the only possibility is to shift unoccupied Fe($3d$) states, similar to the scenario considered in Sec. V A. However, as we have argued, the total change of the electronic structure in this regime does not explain the local stability of the FiM phase. Another direction, associated with the downward shift of the ↑-spin Fe(e_g) band, like in the LSDA(x) approach in Fig. 3, contradicts with the experimental optical data.

Positions of the experimental peaks of the optical conductivity can be adjusted to some extent by considering the breathing distortion *in the direction of Fe atoms* (Fig. 12). However, this scenario would imply a very large distortion $d_{\text{Fe-O}}/d_{\text{Fe-Mo}}<0.475$. As it was already discussed in Sec. V B, there is some controversy about the direction and the magnitude of the breathing distortion in Sr_2FeMoO_6. The optical data depicted in Fig. 12, and also the fact that the distortion $d_{\text{Fe-O}}/d_{\text{Fe-Mo}}<0.475$ easily stabilizes the FiM ordering, might support the conclusion of Ref. 22, but will contradict many others.[4,35,37] Presumably, even if such a distortion does take place in some compounds, it does not operate alone and should be considered in combination with other factors, such as the antisite disorder.

The antisite defects can cause some redistribution of the optical spectra in the direction compatible with the experimental data. At the present stage we cannot calculate the conductivity for disordered alloys. Instead, we discuss the difference of $\sigma(\omega)$ obtained in the supercell calculations for the state A (see Sec. V C) and for the ordered Sr_2FeMoO_6 in the FiM state (Fig. 13). The antisite defects shift the spectral weight from the region of charge transfer excitations around 4.7 eV and from two additional spectral structures around 0.5 and 2.5 eV. The first one is in a good agreement with the experimental data reported in Refs. 4 and 35, and the second one may be related to an additional 2-eV structure observed by Moritomo *et al.* (Ref. 35, see Fig. 11).

The behavior of the optical conductivity in the small-ω region strongly depends on the sample purity. Below we argue that the behavior expected of the perfectly ordered FiM phase is drastically different from the experimental one. First, the theoretical plasma frequency (ω_p) is related to the Drude weight.[54] The latter is typically small if the Fermi surface is composed only of the t_{2g} bands.[55] Therefore, ω_p should be also small and can be estimated for the hypothetical FiM phase of Sr_2FeMoO_6 as $\omega_p \simeq 0.2$ eV. It is significantly smaller than the experimental value $\omega_p \approx 1$ eV,[4] which is also implied in the analysis of magneto-optical spectra.[56,57] Second, according to the experimental data,[4] Sr_2FeMoO_6 exhibits the anomalous Hall effect. The corresponding conductivity can be estimated as $\text{Re}[\sigma_{xy}(0)] \simeq -5\ \Omega^{-1}\text{cm}^{-1}$,[58] which is weaker than the theoretical conductivity ($\text{Re}[\sigma_{xy}(0)] \simeq -19$ and $-10\ \Omega^{-1}\,\text{cm}^{-1}$ correspondingly for the [0,0,1] and [1,1,1] direction of the spin magnetization) by at least factor 2. Therefore, the behavior of the experimental optical conductivity in the small-ω region is largely modified, presumably due to the antisite disorder persisting in the sample.

Finally, we would like to comment on the magneto-optical properties of DP. Generally, the HM ferromagnetic systems are good candidates for magneto-optical applications.[59] This would be true for Sr_2FeMoO_6 and Sr_2FeReO_6, if they were indeed the HM ferrimagnets. On the one hand, these compounds contain heavy elements Mo and Re, which are characterized by large spin-orbit coupling. On

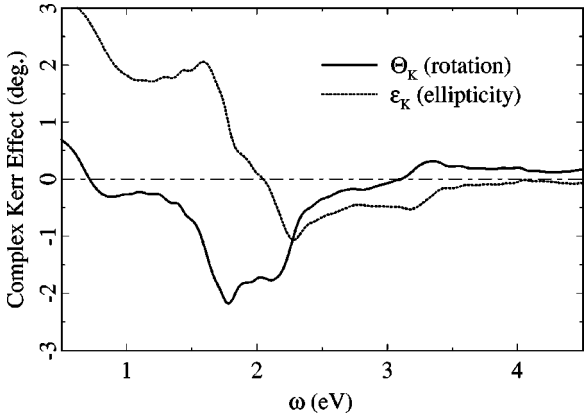

FIG. 14. LSDA calculations of the polar Kerr rotation and Kerr ellipticity spectra for the hypothetical FiM state of Sr_2FeMoO_6.

the other hand, the $\downarrow$-spin t_{2g} states located near ε_F may be the source of large unquenched orbital moment, which is related to the magneto-optical response. The effect can be easily evaluated by including the spin-orbit interaction as a pseudoperturbation in the LMTO method,[19] and calculating the complex polar Kerr effect as

$$\Theta_K + i\epsilon_K = \frac{-\sigma_{xy}(\omega)}{\sigma_{xx}(\omega)\sqrt{1+4\pi i\sigma_{xx}(\omega)/\omega}},$$

with Θ_K and ϵ_K being the Kerr rotation and the Kerr ellipticity, respectively. Results of these calculations for Sr_2FeMoO_6 are shown in Fig. 14. Indeed, one could expect the large Kerr rotation by $-2°$ around 1.8 eV, if the samples were ordered and ferrimagnetic. The experimental situation, however, is not so exciting, and all attempts to measure the polar Kerr rotation in Sr_2FeMoO_6 so far yielded much smaller values of Θ_K: $-0.07°$ at 1.6 eV (Ref. 56) and $-0.45°$ at 1.4 eV (Ref. 57). Therefore, in realistic materials there are some mechanisms that suppress the Kerr effect and presumably destroy the HM character of the electronic structure. Again, from our point of view these mechanisms are most likely to be the antisite disorder and the breathing distortion.

VII. SUMMARY AND DISCUSSIONS

Strong interest to the double perovskite oxides, spurred by potential technological applications of the gigantic magnetoresistance phenomenon subsisting up to the room temperature, is typically linked to their half-metallic electronic structure realized in the ferrimagnetic phase of some ordered compounds, such as Sr_2FeMoO_6 and Sr_2FeReO_6. The analysis of interatomic magnetic interactions presented in our work suggests that this point of view must be largely revised, because the FiM phase appears to be *unstable* and *cannot be* the magnetic ground state of these systems. Ironically, the HM electronic structure itself is the source of this instability as it gives rise to the strong and largely uncompensated AFM superexchange interactions in the system of e_g electrons.

Then, which magnetic ground state is realized in the double perovskites and how one can understand the magnetic behavior of these materials? Below we present our point of view on this problem, which is quite different from others.[2,5–7]

(1) Let us start with Sr_2FeWO_6 that, from our point of view, is a more canonical example of the DP because it is characterized by almost perfect ordering of Fe and W,[11] and its magnetic behavior is less affected by the crystal distortion due to the exceptionally high position of the W(t_{2g}) states relative to ε_F (Sec. V B). Then, according to the analysis of magnetic interactions in Sec. IV, Sr_2FeWO_6 should have a noncollinear spin-spiral ground state. Experimentally, Sr_2FeWO_6 is typically classified as an antiferromagnet with very low Néel temperature.[11,10] However, this assignment is based on the analysis of magnetization data, which cannot exclude the spin-spiral ordering. It would be very interesting to verify our suggestion by using the neutron diffraction.

Another possible candidate for the magnetic ground state of Sr_2FeWO_6 is an inhomogeneous phase separation. According to the electronic structure shown in Fig. 1, the Fe($3d$) states of Sr_2FeWO_6 can be regarded as nearly half filled with a small number of carriers (1/3 electrons per one t_{2g} orbital) doped into the Fe(t_{2g}) band. A very similar picture has been intensively investigated in the context of colossal-magnetoresistive manganites, using a nondegenerate single-band approach.[60,61] Although the single-band description is rather naive for the manganites themselves (for example, the orbital degeneracy in the combination with the double exchange physics presents a crucial factor behind the rich magnetic phase diagram of perovskite manganites—see, e.g., Ref. 18), such an analysis did reveal several fundamental properties of a more general character. Particularly, it is know that the competition between the FM double exchange and the AFM superexchange interaction in fully spin-polarized systems near the half filling often leads to the inhomogeneous phase separation into the ferromagnetically and antiferromagnetically ordered regions. The topological aspect of the phase separation are barely understood and strongly depend on the form of approximation employed for the analysis of the problem. For example, in the local CPA approach for diluted magnetic semiconductors, the tendency towards the phase separation is realized as a spin-glass-like local-moment disordered phase, without a long-range magnetic order.[47,48] Starting with a jellium model, the phase separation would typically result in the formation of FM droplets in an AFM background.[60]

In Sr_2FeWO_6, the ballance towards the phase separation can be easily shifted by introducing additional defects and thereby artificially increasing the inhomogeneity of the sample. For example, the behavior of magnetization in the alloy $Sr_2Fe(W_{1-x}Mo_x)O_6$ in the range of $0 \leqslant x \leqslant 0.4$ as a function of temperature and external magnetic field clearly shows some features of ''spin canting'' associated with a large coercive field.[11] Taking into account the particular electronic structure of the ordered DP, it is more reasonable to assume that these magnetization data indicate at a phase separation, which is difficult to distinguish experimentally from the spin canting.

There are also some indications at the effects of dynamic phase separation at elevated temperatures. First, it seems that

it is very difficult to establish the long-range magnetic order, which may take place only at very low temperatures (below 37 K). Second, the value of effective magnetization $\mu_{\rm eff} = 6.58\mu_B$ derived from the behavior of magnetic susceptibility above the transition temperature is very large and cannot be reconciled with any of the local ionic pictures.[10] This might indicate the formation of some sort of stable FM droplets above T_N.

Finally, the AFM ground state in Sr_2FeWO_6 can be attributed to the Coulomb correlations, in an analogy with FeO.[6] From our point of view this scenario is rather unlikely. First, it relies on fine tuning of the Coulomb repulsion parameter to a great extent, which opens the gap in Sr_2FeWO_6, but not in Sr_2FeMoO_6 or Sr_2FeReO_6. Second, it does not explain the exceptionally low T_N in Sr_2FeWO_6.

(2) The stabilization of the FiM ordering in Sr_2FeMoO_6 or Sr_2FeReO_6 should invoke to an additional mechanism, and most probably be accompanied by demolishing of the HM electronic structure, and a decrease of the saturation magnetization. We have considered two scenarios.

In some cases the FiM ordering can be stabilized by the breathing distortion. This mechanism is especially efficient if oxygens move in the direction of Fe atoms, leading to a partial depopulation of the majority-spin Fe(e_g) band and activating the new channel for the strong FM double exchange interactions associated with the e_g electrons, similar to the colossal-magnetoresistive manganites. Taking into account the experimental directions of the breathing distortion in the DP,[4,12,35,37] one may expect this mechanism to play some role in Sr_2FeReO_6.

In partially disordered compounds, the FiM ordering can be stabilized by AFM SE interactions between Fe atoms located at the ideal and antisite positions. This mechanism is extremely efficient. For example, by taking into account only the SE interactions in the system of e_g electrons, the FiM ordering can be stabilized by less than 10% of antisite defects. Note also that the antisite defects will deteriorate mobility of the minority-spin t_{2g} electrons, in some analogy with the effect of disorder on the properties of ferromagnetic manganites.[62] This might explain the fact that some of the ferrimagnetically ordered DP, like Ca_2FeReO_6, are *insulators*,[12] though the details of this phenomenon are presumably rather complicated and may involve not only the antisite disorder but also the disorder of local lattice distortions induced by a smaller size of Ca^{2+} ions. We would like to emphasize also that the difference between Sr_2FeReO_6 and Ca_2FeReO_6 cannot be attributed to the chemical difference between Sr^{2+} and Ca^{2+} ions. For example, similar calculations for the doped manganites show that once the crystal structure is fixed, the exact type of the dopant (Ca, Sr, or Ba) has only a little effect on the electronic structure and electronic properties. This is also supported by calculations of magnetic interactions in Sr_2FeMoO_6 and Ba_2FeMoO_6 (Table II), which are practically identical if one considers the same (cubic) crystal structure.

When the number of antisite defects increases, the main mechanism responsible for the stability of the FiM ordering switches from the generalized double exchange, operating in the conduction t_{2g} band, to the AFM superexchange with impurity Fe sites. The latter is more robust and may explain stability of the FiM phase in the wide range of defect concentrations varying from only few percents, when the t_{2g} states remain metallic, and until high concentrations, which may destroy the metallic behavior. If this scenario is correct, there should be some optimal concentration of the antisite defect, which (on the one hand) is sufficiently large to stabilize the FiM phase, and (on the other hand) is sufficiently low to preserve mobility of the t_{2g} electrons and rather high-saturation magnetization, which are required for the magnetoresistive behavior.

Our analysis of the antisite disorder is based on a simple model description, which illustrates only the main idea. As the next step it would be very important to gain a quantitative description of effects of the antisite disorder on the electronic and magnetic properties of DP by using the first-principles CPA method.[46–48]

ACKNOWLEDGMENTS

I would like to thank K. Terakura, Y. Tomioka, Z. Fang, Y. Tokura, N. Hamada, and N. Nagaosa for fruitful discussions; Y. Okimoto and Y. Moritomo for providing the numerical information of experimental optical spectra published in Refs. 4 and 35; H. Kato for providing unpublished results;[12] and I. A. Abrikosov for providing unpublished results[48] prior to publication. The present work was partly supported by New Energy and Industrial Technology Development Organization (NEDO).

*Electronic address: igor.solovyev@aist.go.jp

[1] J. Longo and R. Word, J. Am. Chem. Soc. **83**, 2816 (1961); F.K. Patterson, C.W. Moeller, and R. Word, Inorg. Chem. **2**, 196 (1963); A.W. Sleight and J.F. Weiher, J. Phys. Chem. Solids **33**, 679 (1972).

[2] K.-I. Kobayashi, T. Kimura, H. Sawada, K. Terakura, and Y. Tokura, Nature (London) **395**, 677 (1998).

[3] K.-I. Kobayashi, T. Kimura, Y. Tomioka, H. Sawada, K. Terakura, and Y. Tokura, Phys. Rev. B **59**, 11 159 (1999).

[4] Y. Tomioka, T. Okuda, Y. Okimoto, R. Kumai, K.-I. Kobayashi, and Y. Tokura, Phys. Rev. B **61**, 422 (2000).

[5] D.D. Sarma, P. Mahadevan, T. Saha-Dasgupta, S. Ray, and A. Kumar, Phys. Rev. Lett. **85**, 2549 (2000).

[6] Z. Fang, K. Terakura, and J. Kanamori, Phys. Rev. B **63**, 180407 (2001).

[7] J. Kanamori and K. Terakura, J. Phys. Soc. Jpn. **70**, 1433 (2001).

[8] Ll. Balcells, J. Navarro, M. Bibes, A. Roig, B. Martínez, and J. Fontcuberta, Appl. Phys. Lett. **78**, 781 (2001).

[9] According to the magnetic circular x-ray dichroism measurements, the orbital magnetic moments are rather small. For example, in Sr_2FeMoO_6 one expects $\mu_{\rm spin}({\rm Fe}) \simeq 2.9\mu_B$, $\mu_{\rm orb}({\rm Fe}) \simeq 0.1\mu_B$, and $\mu_{\rm orb}({\rm Mo}) \simeq -0.15\mu_B$. However, it is important that $\mu_{\rm orb}$(Fe) is finite and parallel to $\mu_{\rm spin}$(Fe). According to Hund's third rule, this means that the number of Fe($3d$) electrons should be larger than five, and the formal ionization state of Fe in Sr_2FeMoO_6 is between Fe^{3+} and Fe^{2+} (T. Koide *et al.*,

unpublished and private communication).
[10] H. Kawanaka, I. Hase, S. Toyama, and Y. Nishihara, J. Phys. Soc. Jpn. **68**, 2890 (1999).
[11] K.-I. Kobayashi, T. Okuda, Y. Tomioka, T. Kimura, and Y. Tokura, J. Magn. Magn. Mater. **218**, 17 (2000).
[12] H. Kato, T. Okuda, Y. Okimoto, Y. Tomioka, K. Oikawa, T. Kamiyama, and Y. Tokura (unpublished).
[13] A.I. Liechtenstein, M.I. Katsnelson, V.P. Antropov and, V.A. Gubanov, J. Magn. Magn. Mater. **67**, 65 (1987).
[14] W.E. Pickett, Phys. Rev. B **57**, 10 613 (1998).
[15] K. Miura and K. Terakura, Phys. Rev. B **63**, 104402 (2001).
[16] I.V. Solovyev and K. Terakura, Phys. Rev. B **58**, 15496 (1998).
[17] I.V. Solovyev and K. Terakura, Phys. Rev. B **63**, 174425 (2001).
[18] I. V. Solovyev and K. Terakura, in *Electronic Structure and Magnetism of Complex Materials*, edited by D. J. Singh (Springer-Verlag, Berlin, 2002).
[19] O.K. Andersen, Phys. Rev. B **12**, 3060 (1975); O. Gunnarsson, O. Jepsen, and O.K. Andersen, Phys. Rev. B **27**, 7144 (1983).
[20] L.M. Sandratskii, Phys. Status Solidi B **136**, 167 (1986); O.N. Mryasov, A.I. Liechtenstein, L.M. Sandratskii, and V.A. Gubanov, J. Phys.: Condens. Matter **3**, 7683 (1991); S.V. Halilov, H. Eschrig, A.Y. Perlov, and P.M. Oppeneer, Phys. Rev. B **58**, 293 (1998).
[21] Formally, the interactions between the Fe and *M* sublattices can be found by using the same procedure as in the model tight-binding analysis in Sec. V D, but in practical terms the calculations are rather heavy.
[22] Y. Moritomo, Sh. Xu, T. Akimoto, A. Machida, N. Hamada, K. Ohoyama, E. Nishibori, M. Takata, and M. Sakata, Phys. Rev. B **62**, 14 224 (2000).
[23] I.V. Solovyev and K. Terakura, Phys. Rev. Lett. **82**, 2959 (1999).
[24] K. Terakura, T. Oguchi, A.R. Williams, and J. Kübler, Phys. Rev. B **30**, 4734 (1984).
[25] The difference is related to the fact that the $pd\sigma$ hoppings in the cubic lattice are much stronger than the $pd\pi$ ones–see, e. g., T. Mizokawa and A. Fujimori, Phys. Rev. B **51**, 12 880 (1995).
[26] According to Eq. (2), parameters of magnetic interactions depend on the details of the electronic structure of the magnetic state in which they are calculated. This dependence enters Eq. (2) both through the intra-atomic exchange splittings $\Delta_{\rm ex}$ and the inter-atomic elements of the one-electron Green function $\hat{\mathcal{G}}$. Since the electronic structure of the DP is very different in the FiM and type-II AFM phases (Fig. 1), it is reasonable to expect also very different behavior of the magnetic interactions in these two states.
[27] R.O. Jones and O. Gunnarsson, Rev. Mod. Phys. **61**, 689 (1989); F. Aryasetiawan and O. Gunnarsson, Rep. Prog. Phys. **61**, 237 (1998).
[28] If it is not specified otherwise, we used the exchange-correlation potential by S.H. Vosko, L. Wilk, and M. Nusair, Can. J. Phys. **58**, 1200 (1980).
[29] J.P. Perdew and W. Yue, Phys. Rev. B **33**, 8800 (1986); J.P. Perdew, *ibid.* **33**, 8822 (1986).
[30] O. Gunnarsson, J. Phys. F: Met. Phys. **6**, 587 (1976).
[31] V.I. Anisimov, J. Zaanen, and O.K. Andersen, Phys. Rev. B **44**, 943 (1991).
[32] J. Zaanen and G.A. Sawatzky, Can. J. Phys. **65**, 1262 (1987).
[33] K. Terakura, Z. Fang, and I. V. Solovyev, in *Physics and Chemistry of Transition-Metal Oxides*, edited by H. Fukuyama and N. Nagaosa (Springer-Verlag, Berlin, 1999), p. 34.
[34] D.D. Sarma, N. Shanthi, S.R. Barman, N. Hamada, H. Sawada, and K. Terakura, Phys. Rev. Lett. **75**, 1126 (1995).
[35] Y. Moritomo, Sh. Xu, A. Machida, T. Akimoto, E. Nishibori, M. Takata, and M. Sakata, Phys. Rev. B **61**, R7827 (2000).
[36] Of course, another interesting regime is when U_M is larger than the Mo(t_{2g}) bandwidth ($\sim$1.7 eV). It may produce the spontaneous orbital polarization, open the band gap, and in principle give rise to the rich variety of orbital phenomena (for example, the ones anticipated in Ref. 12). It might be a possible scenario for insulating Ca_2FeReO_6 (Ref. 12, though another alternative may be the antisite disorder combined with the disorder of local lattice distortions, which is discussed in Sec. VII), but presumably not for metallic Sr_2FeMoO_6.
[37] O. Chmaissem, R. Kruk, B. Dabrowski, D.E. Brown, X. Xiong, S. Kolesnik, J.D. Jorgensen, and C.W. Kimball, Phys. Rev. B **62**, 14 197 (2000).
[38] For example, the SE interaction between two *d* orbitals and mediated by one oxygen *p* orbital is given by $J^S = -(t_{pd}^4/\Delta_{\rm ct}^2)(1/\Delta_{\rm ex}+1/\Delta_{\rm ct})$, where $\Delta_{\rm ct}$ is the charge-transfer energy and t_{pd} is the *p*-*d* transfer integral (Ref. 32).
[39] Y. Moritomo, N. Shimamoto, Sh. Xu, A. Machida, E. Nishibori, M. Takata, M. Sakata, and A. Nakamura, Jpn. J. Appl. Phys., Part 2 **40**, L672 (2001).
[40] K. Terakura (unpublished).
[41] T. Saha-Dasgupta and D.D. Sarma, Phys. Rev. B **64**, 064408 (2001).
[42] In fact, the convergence was rather bad both for the F and A types of defects. In order to stabilize it we had to use a very small mixing parameter for the LSDA potential. Perhaps even better solution in such a situation would be to use the fixed-spin-moment method [V.L. Moruzzi, Phys. Rev. Lett. **57**, 2211 (1986)]. Note also that there is a clear physical reason why two different solutions should coexist: Fe has a robust local magnetic moment that does not collapse even if one changes its direction with respect to the hosts. Moreover, both F and A are the collinear spin states, in which there are no rotational forces acting to flip the Fe spin. Therefore, both of them should be equilibrium points of the total energy.
[43] J.C. Slater and G.F. Koster, Phys. Rev. **94**, 1498 (1954).
[44] P. W. Anderson, in *Solid State Physics*, edited by F. Zeitz and D. Turnbull (Academic, New York, 1963), Vol. 14, p. 99.
[45] C.M. Varma, Phys. Rev. B **54**, 7328 (1996).
[46] P. Soven, Phys. Rev. **156**, 809 (1967); J.S. Faulkner and G.M. Stocks, Phys. Rev. B **21**, 3222 (1980); A.V. Ruban, I.A. Abrikosov, and H.L. Skriver, *ibid.* **51**, 12 958 (1995).
[47] H. Akai, Phys. Rev. Lett. **81**, 3002 (1998).
[48] P.A. Korzhavyi, I.A. Abrikosov, E.A. Smirnova, L. Bergqvist, P. Mohn, R. Mathieu, P. Svedlindh, J. Sadowski, E.I. Isaev, Yu.Kh. Vekilov, and O. Eriksson (unpupblished).
[49] L.N. Bulaevskii and S.V. Panyukov, Pis'ma Zh. Eksp. Teor. Fiz. **43**, 190 (1986) [JETP Lett. **43**, 240 (1986)]; P.M. Levy, S. Maekawa, and P. Bruno, Phys. Rev. B **58**, 5588 (1998).
[50] Note that the tight-binding model is designed only for the e_g states and does not take into account the DE contributions coming from the metallic t_{2g} bands. Therefore, both $J_1^{\rm Fe\text{-}Fe}$ and $J_2^{\rm Fe\text{-}Fe}$ are negative. Then, the inequality $|J_1^{\rm Fe\text{-}Fe}|>|J_2^{\rm Fe\text{-}Fe}|$ is an artifact of the *s*-orbital description for the SE interactions. Taking into account the realistic form of the transfer integrals between two

e_g orbitals in the cubic lattice (Ref. 43), one could get the opposite trend $|J_1^{\text{Fe-Fe}}|<|J_2^{\text{Fe-Fe}}|$. However, this difference will not change the main conclusions of our model tight-binding analysis about the local stability of the FiM state.

[51] Y. Okimoto (private communication).

[52] The calculations of optical properties are based on the Kubo formalism, the implementation of which is similar to our previous work on manganites (see Ref. 18 for a review). The Brillouin zone integration has been replaced by a summation over the mesh of $40\times40\times40$ **k** points with the Lorentzian broadening $\eta=68$ meV.

[53] I. Solovyev, N. Hamada, and K. Terakura, Phys. Rev. B **53**, 7158 (1996).

[54] See, e.g., Ref. 18 and references therein.

[55] This is also true for some other t_{2g} systems, e.g., Fe_3O_4: A. Yanase and N. Hamada, J. Phys. Soc. Jpn. **68**, 1607 (1999).

[56] U. Rüdiger, M. Rabe, G. Güntherodt, H.Q. Yin, R.I. Dass, and J.B. Goodenough, Appl. Phys. Lett. **77**, 2216 (2000).

[57] T. Kise, T. Ogasawara, M. Ashida, Y. Tomioka, Y. Tokura, and M. Kuwata-Gonokami, Phys. Rev. Lett. **85**, 1986 (2000).

[58] According to the experimental data in Ref. 4, the anomalous Hall coefficient for the Sr_2FeMoO_6 single crystal is $R_s\simeq1.16\times10^{-10}$ Ω cm/G, and the magnetization is $\mu\simeq2802$ G. Then, the Hall resistivity extrapolated to $T=0$ and $H=0$ can be estimated as $\rho_{xy}=R_s\mu\simeq0.325\times10^{-6}$ Ω cm. Taking into account that the (normal) resistivity is $\rho_0\simeq0.27\times10^{-3}$ Ω cm (Refs. 4,39), the anomalous Hall conductivity can be estimated as $\mathrm{Re}[\sigma_{xy}(0)]\simeq-\rho_{xy}/\rho_0^2\simeq-5$ $\Omega^{-1}\,\mathrm{cm}^{-1}$.

[59] V.Yu. Irkhin and M.I. Katsnel'son, Phys. Usp. **37**, 659 (1994).

[60] E.L. Nagaev, Phys. Usp. **38**, 497 (1995); **39**, 781 (1996).

[61] E. Dagotto, S. Yunoki, A.L. Malvezzi, A. Moreo, J. Hu, S. Capponi, D. Poilblanc, and N. Furukawa, Phys. Rev. B **58**, 6414 (1998); A. Moreo, S. Yunoki, and E. Dagotto, Science **283**, 2034 (1999).

[62] W.E. Pickett and D.J. Singh, Phys. Rev. B **55**, R8642 (1997).